Euro. Jnl of Applied Mathematics (2002), *vol.* 13, *pp.* 225–259.
DOI: 10.1017/S0956792501004636 Printed in the United Kingdom

Multiphase flow in a roll press nip

A. D. FITT [1], P. D. HOWELL [2], J. R. KING [2], C. P. PLEASE [1] and D. W. SCHWENDEMAN [3]

[1] *Faculty of Mathematical Studies, University of Southampton, Southampton SO17 1BJ, UK*
[2] *School of Mathematical Sciences, University of Nottingham, University Park, Nottingham NG7 2RD, UK*
[3] *Department of Mathematical Sciences, Rensselaer Polytechnic Institute, Troy, NY 12180, USA*

(*Received 18 September 2000; revised 2 May 2001*)

A three-phase ensemble-averaged model is developed for the flow of water and air through a deformable porous matrix. The model predicts a separation of the flow into saturated and unsaturated regions. The model is closed by proposing an experimentally-motivated heuristic elastic law which allows large-strain nonlinear behaviour to be treated in a relatively straightforward manner. The equations are applied to flow in the 'nip' area of a roll press machine whose function is to squeeze water out of wet paper as part of the manufacturing process. By exploiting the thin-layer limit suggested by the geometry of the nip, the problem is reduced to a nonlinear convection-diffusion equation with one free boundary. A numerical method is proposed for determining the flow and sample simulations are presented.

1 Introduction

1.1 Industrial background

This study is concerned with the dynamics of a 'roll press nip', a crucial component in the manufacture of paper. A typical paper-making process is divided into three steps: forming, pressing and drying. In the forming section, raw materials are combined to form a wet paper mixture. The priority is then to remove the maximum amount of water without affecting the structural integrity of the paper. The key requirement of the press section is that water removal should be via mechanical means, for the thermal drying employed later in the process is much more expensive when the water content of the paper is high.

The basic function of the press section of a paper-making machine, and the process we wish specifically to study, involves squeezing of the paper between two rollers. This happens many times and in many different ways to a single portion of the paper sheet; we shall examine a single pass through such a 'roll press nip'. A great deal of water is removed by this process. Typically on first entry into the pressing section the paper consists of 20% fibre and 80% water, and the water content is reduced by around a quarter at each pass through the nip. The remaining water is then removed by the drying section of the machine, after which the paper comprises roughly 5% water.

A schematic diagram of a roll press nip is shown in Figure 1. The two steel rollers are typically each about 1m in diameter. The just-formed paper (usually about 0.5mm thick) enters the nip seated on a fabric sheet hereinafter referred to as 'felt'. The felt is

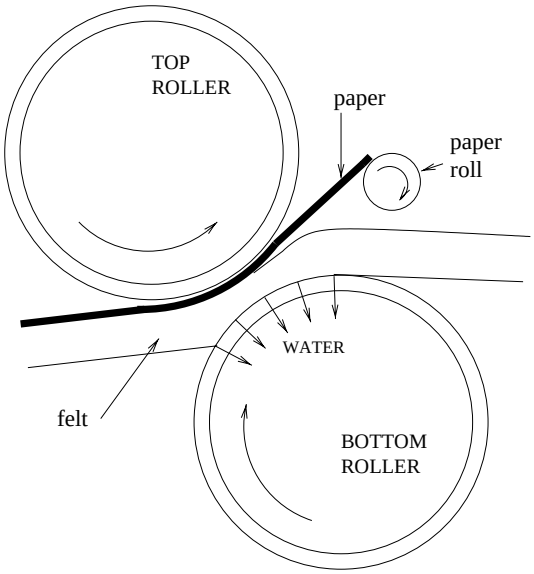

FIGURE 1. Schematic diagram of typical roll press nip.

composed of woven nylon textile fibres; it may be regarded as a porous medium that, in its undeformed state, is about 3mm thick. Before deformation under the rollers, the felt has a solid volume fraction of about 50%; during loading, this may increase to 80%. As the paper sheet and fabric enter the nip region, both are compressed. During compression the fabric structure deforms and the water is squeezed out of the paper and the fabric. Although a number of different arrangements are possible, it is usual for the bottom roller to possess holes or slots through which water can pass. Thus, any water that is squeezed out of the bottom of the felt is removed altogether. After the squeezing has taken place, the felt is removed by the bottom roller; the paper remains in contact with the top roller for a little longer, and is then wound onto a smaller paper roller while the felt travels in a closed loop. A typical feed speed is about 20m/s and the pressure under the rollers may reach 10MPa. Of course, a roll press is a very complicated item of equipment and we have indicated only its main features; the interested reader may find more details in Reese [15].

1.2 Modelling objectives

In the industrial context, the size and speed of a roll press machine, not to mention the expense involved in interrupting the process, make it very difficult to take direct measurements. The distribution of pressure, velocity and felt porosity in the nip have therefore traditionally been matters of great debate. In this study, we do not attempt to answer any one specific question, but rather wish to propose a general framework for modelling the flow in a roll press nip. In this way we aim to develop a thorough theoretical understanding whereby the processes involved may be optimised. We address the problem using a three-phase flow approach, aiming initially to include all the effects that might be important and then making clearly defined assumptions to simplify the equations. Thus

the formulation that is developed may readily be extended to other liquid/air poroelastic problems.

2 Three-phase flow modelling

2.1 Preamble

Throughout this study we consider three phases of which two (water and air) are fluid and one (felt) is solid; in other words, we do not explicitly attempt to model the paper phase. The intention is that any modelling applied to the felt should also, with a suitable modification of the material properties, apply to paper. In any case, the paper layer is somewhat thinner than the felt, and is thought to play a passive role in the process, so our main priority is to determine the water and air distribution in the felt. In § 2.2 we develop a three-phase flow model in a general form, before introducing simplifications and constitutive assumptions specific to paper making in § 2.3–2.4, and presenting the final simplified equations in § 2.5.

Many previous models have been proposed for the flow of liquid in a deformable porous medium. The original motivation for such studies was the need to understand the settlement of soils. The first major contributions to this area seem to have been by Terzaghi [17] and Biot [2]. Biot noted the similarity between the processes of soil consolidation and the squeezing of water out of a 'saturated rubber sponge'. Linear elasticity, Darcy's law and conservation of mass were used in Biot [2] to yield a single equation for the strains of the combined porous medium/water mixture. The theory was later extended to anisotropic porous media [3]. Biot theory of this form is essentially a mixture theory (see, for example, Atkin & Craine [1]), in which no attempt is made to write down equations for each phase of the system. It has since been generalised to include effects such as coupled heat and moisture transfer [11], and may be formulated in a convenient way for numerical solution (see, for example, Cheng & Detourney [5]). Biot theory models have also been applied in a medical context [12, 13] to the compression of soft tissue.

Here we adopt a rather different modelling approach, in which the problem is treated as a multiphase flow (see, for example, Drew [6] and Lai & Mow [10]). The solid, liquid and air (if present) are all treated as separate phases and ensemble-averaged equations are proposed for each phase. Although this method may be thought of as being more rigorous than the mixture approach, it is frequently more difficult to make the correct constitutive assumptions to close the model.

The spontaneous relaxation of a compressed wet sponge and the infiltration of an incompressible liquid into an initially dry or partially dry sponge was studied in Preziosi *et al.* [14] from a multiphase flow viewpoint. Assuming a constitutive law based on uniaxial stress/strain tests, a nonlinear diffusion equation was derived for the flow. A related approach was used in Spiegelman [16], where low viscosity fluid flowing in a deformable permeable matrix was modelled. A 'single pressure' assumption led to a system of partial differential equations in which the shear deformation of the matrix is governed by Stokes' equations and the porosity satisfies a nonlinear dispersive wave equation.

2.2 The general equations

Guided by the above literature, we propose an ensemble-averaged multiphase model which will be applied to the flow in a roll press nip. We denote the water (liquid), air and felt velocities by $\boldsymbol{q}_\ell$, $\boldsymbol{q}_a$ and $\boldsymbol{q}_f$ respectively; all are functions of spatial position $\boldsymbol{x}$ and time t. The equations representing conservation of mass and momentum for the liquid, air and felt respectively (for a derivation see, for example, Drew & Wood [7]) are

$$(\rho_\ell \alpha)_t + \nabla.(\rho_\ell \alpha \boldsymbol{q}_\ell) = 0, \tag{2.1}$$

$$(\rho_a \beta)_t + \nabla.(\rho_a \beta \boldsymbol{q}_a) = 0, \tag{2.2}$$

$$(\rho_f \gamma)_t + \nabla.(\rho_f \gamma \boldsymbol{q}_f) = 0, \tag{2.3}$$

$$(\rho_\ell \alpha \boldsymbol{q}_\ell)_t + \nabla.(\rho_\ell \alpha \boldsymbol{q}_\ell \boldsymbol{q}_\ell) = \nabla.(\alpha(\boldsymbol{T}_\ell + \boldsymbol{T}_\ell^{Re})) + \alpha \rho_\ell \boldsymbol{b} + \boldsymbol{M}_\ell, \tag{2.4}$$

$$(\rho_a \beta \boldsymbol{q}_a)_t + \nabla.(\rho_a \beta \boldsymbol{q}_a \boldsymbol{q}_a) = \nabla.(\beta(\boldsymbol{T}_a + \boldsymbol{T}_a^{Re})) + \beta \rho_a \boldsymbol{b} + \boldsymbol{M}_a, \tag{2.5}$$

$$(\rho_f \gamma \boldsymbol{q}_f)_t + \nabla.(\rho_f \gamma \boldsymbol{q}_f \boldsymbol{q}_f) = \nabla.(\gamma(\boldsymbol{T}_f + \boldsymbol{T}_f^{Re})) + \gamma \rho_f \boldsymbol{b} + \boldsymbol{M}_f. \tag{2.6}$$

Here the densities of the liquid, air and felt are denoted by ρ_ℓ, ρ_a and ρ_f respectively. The volume fraction of liquid is α, the fraction of air β, and the solid fraction γ; phase contiguity implies that

$$\alpha + \beta + \gamma \equiv 1. \tag{2.7}$$

The applied body force is represented by $\boldsymbol{b}$. The stress tensors of the liquid, air and felt are written as $\boldsymbol{T}_\ell$, $\boldsymbol{T}_a$ and $\boldsymbol{T}_f$, respectively, whilst the corresponding stress tensors arising from Reynolds' stresses are denoted by $\boldsymbol{T}_\ell^{Re}$, $\boldsymbol{T}_a^{Re}$ and $\boldsymbol{T}_f^{Re}$. The $\boldsymbol{M}_k$ ($k = \ell$, a or f) denote the interfacial momentum source terms.

Equations (2.1)–(2.6) (which have become the recognised starting point for models of many different multiphase flow regimes) are posed entirely in terms of *ensemble-averaged* variables, the ensemble average $< f >$ of a field $f(\boldsymbol{x}, t)$ being defined by

$$< f >= \int_M f(\boldsymbol{x}, t; \zeta) d\mu(\zeta), \tag{2.8}$$

where $\mu(\zeta)$ in (2.8) is the probability density of observing the result ζ and M the set of all such results. Space does not permit a discussion of the effects of averaging on the equations, but it is worth noting that (a) the $\boldsymbol{M}_k$ terms are a direct result of the averaging process and (b) all profile coefficients (terms arising from the fact that the product of the average is not equal to the average of the product) have been set to unity.

It is now necessary to make some further assumptions to proceed. It has become normal (see, for example, Drew & Wood [7]) to write

$$\boldsymbol{M}_\ell = p_{\ell i} \nabla \alpha + \boldsymbol{M}'_\ell$$

(with similar definitions for $\boldsymbol{M}_a$ and $\boldsymbol{M}_f$), where p_{ki} is the interfacially-averaged pressure of phase k and the $\boldsymbol{M}'_k$ contain all terms related to drag, virtual mass, Bassett and Faxen forces and any other unsteady flow effects that might be important. In this case, we ignore all such effects except for the interphase drag forces, and denote the drag force per unit volume on phase j due to phase k by $\boldsymbol{D}_{jk}$; Newton's third law implies that $\boldsymbol{D}_{jk} \equiv -\boldsymbol{D}_{kj}$. We will later propose models for the drag forces which account for all the important effects of viscosity, and thus in the liquid and air phases the stress tensors are given

https://doi.org/10.1017/S0956792501004636 Published online by Cambridge University Press

by $\boldsymbol{T}_\ell = -p_\ell \boldsymbol{I}$ and $\boldsymbol{T}_a = -p_a \boldsymbol{I}$ respectively. Additionally, since the liquid and air flow through a porous medium, the flow is assumed to be laminar, so there are no Reynolds' stress terms. The only body force that we shall consider is gravity.

We treat both the water and the air as incompressible: the compressibility of the water is certainly negligible and, despite the large roller pressures alluded to earlier, compressibility effects in the air may be ignored owing to the high mobility of the air. Compression of the felt is assumed to occur through deformation of the matrix rather than of the elastic material from which the fibres are formed. Thus the solid phase is likewise treated as incompressible.

Next, for simplicity we set the bulk pressure in each phase equal to the interfacial pressure. Though it is well-established that this assumption may lead to serious errors in inertia-dominated flows (including change-of-type difficulties; see, for example, Fitt [9]), no such problems arise when inertia is negligible, as will turn out to be the case here. A further assumption must be made concerning the pressures: we set the phasic bulk pressures equal so that $p_\ell = p_a = p_f = p$. This assumption is tantamount to ignoring any surface energy effects (these could easily be incorporated into the model if desired). Finally, we write the felt stress tensor $\boldsymbol{T}_f$ in the form

$$\gamma \boldsymbol{T}_f = -\gamma p_f \boldsymbol{I} + \boldsymbol{\tau}_f, \tag{2.9}$$

where the felt deviatoric stress tensor $\boldsymbol{\tau}_f$ accounts for stress not due to pressure, i.e. that due to felt deformation. The definition (2.9) means that $\boldsymbol{\tau}_f$ is the elastic stress in the felt averaged across the area occupied by all three phases. Put another way, $\boldsymbol{\tau}_f$ is the stress tensor one would measure for the solid matrix as a whole in the absence of the other two phases.

Finally, then, the generic equations are

$$\alpha_t + \nabla.(\alpha \boldsymbol{q}_\ell) = 0, \tag{2.10}$$

$$\beta_t + \nabla.(\beta \boldsymbol{q}_a) = 0, \tag{2.11}$$

$$\gamma_t + \nabla.(\gamma \boldsymbol{q}_f) = 0, \tag{2.12}$$

$$\rho_\ell(\alpha \boldsymbol{q}_\ell)_t + \rho_\ell \nabla.(\alpha \boldsymbol{q}_\ell \boldsymbol{q}_\ell) = -\alpha \nabla p + \alpha \rho_\ell \boldsymbol{g} + \boldsymbol{D}_{\ell a} + \boldsymbol{D}_{\ell f}, \tag{2.13}$$

$$\rho_a(\beta \boldsymbol{q}_a)_t + \rho_a \nabla.(\beta \boldsymbol{q}_a \boldsymbol{q}_a) = -\beta \nabla p + \beta \rho_a \boldsymbol{g} - \boldsymbol{D}_{\ell a} + \boldsymbol{D}_{af}, \tag{2.14}$$

$$\rho_f(\gamma \boldsymbol{q}_f)_t + \rho_f \nabla.(\gamma \boldsymbol{q}_f \boldsymbol{q}_f) = -\gamma \nabla p + \nabla.\boldsymbol{\tau}_f + \gamma \rho_f \boldsymbol{g} - \boldsymbol{D}_{\ell f} - \boldsymbol{D}_{af}. \tag{2.15}$$

If the drag forces and $\boldsymbol{\tau}_f$ were known as functions of the other dependent variables then (2.10)–(2.11) would constitute $1 + 1 + 1 + 3 + 3 + 3 = 12$ equations in the 12 unknowns α, β, p, $\boldsymbol{q}_\ell$, $\boldsymbol{q}_a$ and $\boldsymbol{q}_f$. The formulation is thus nominally complete.

2.3 Dimensional analysis

We now non-dimensionalise equations (2.10)–(2.15) to determine which of the terms are significant. Thus by eliminating all negligible effects we arrive at a considerably simplified model. For the moment we use the equilibrium felt thickness h_i as a characteristic length-scale; the fact that the region in which the felt is squeezed by the rollers is long compared with h_i will be exploited in § 3. The feed speed u_∞ of the felt is used as a typical velocity.

Detailed modelling of the elastic behaviour of the felt and of the interphase drag terms

https://doi.org/10.1017/S0956792501004636 Published online by Cambridge University Press

Table 1. *Typical parameter values for a roll press nip*

Property	Symbol	Approximate value	Units
Water density	ρ_ℓ	10^3	$\mathrm{Kg\,m^{-3}}$
Water viscosity	ν_ℓ	10^{-6}	$\mathrm{m^2 s^{-1}}$
Air density	ρ_a	1	$\mathrm{Kg\,m^{-3}}$
Air viscosity	ν_a	10^{-5}	$\mathrm{m^2 s^{-1}}$
Felt density	ρ_f	10^3	$\mathrm{Kg\,m^{-3}}$
Felt elastic modulus	E	10^7	Pa
Roller radius	R	0.5	m
Gap thickness	h_0	2×10^{-3}	m
Undeformed felt thickness	h_i	3×10^{-3}	m
Felt pore size	a	10^{-6}	m
Felt speed	u_∞	20	$\mathrm{m\,s^{-1}}$

will be carried out in section 2.4. For the moment we characterise $\boldsymbol{\tau}_f$ by a typical elastic modulus E, and estimate $\boldsymbol{D}_{\ell a}$, $\boldsymbol{D}_{\ell f}$ and $\boldsymbol{D}_{af}$ using a viscous drag law based on the pore size a. Thus we non-dimensionalise (2.10)–(2.15) as follows:

$$\begin{aligned} \boldsymbol{x} &= h_i \boldsymbol{x}^*, & t &= (h_i/u_\infty)\, t^*, \\ \boldsymbol{q}_\ell &= u_\infty \boldsymbol{q}_\ell^*, & \boldsymbol{q}_a &= u_\infty \boldsymbol{q}_a^*, \\ \boldsymbol{q}_f &= u_\infty \boldsymbol{q}_f^*, & p &= E p^*, \\ \boldsymbol{\tau}_f &= E \boldsymbol{\tau}_f^*, & \boldsymbol{D}_{\ell a} &= (\rho_a \nu_a u_\infty / a^2)\, \boldsymbol{D}_{\ell a}^*, \\ \boldsymbol{D}_{\ell f} &= (\rho_\ell \nu_\ell u_\infty / a^2)\, \boldsymbol{D}_{\ell f}^*, & \boldsymbol{D}_{af} &= (\rho_a \nu_a u_\infty / a^2)\, \boldsymbol{D}_{af}^*, \end{aligned}$$

where ν_a and ν_ℓ are the kinematic viscosities of water and air respectively. Notice that these scaling estimates justify *a posteriori* our neglect of the viscous terms in $\boldsymbol{T}_a$ and $\boldsymbol{T}_\ell$: since the pore size a is very much smaller than any other length-scale in the problem, the interphase drag necessarily dominates any macroscopic viscous effects.

We henceforth drop the asterisks for ease of notation. Then the dimensionless equations are

$$\begin{aligned} \alpha_t + \nabla.(\alpha \boldsymbol{q}_\ell) &= 0, \\ \beta_t + \nabla.(\beta \boldsymbol{q}_a) &= 0, \\ \gamma_t + \nabla.(\gamma \boldsymbol{q}_f) &= 0, \\ \Theta_\ell[(\alpha \boldsymbol{q}_\ell)_t + \nabla.(\alpha \boldsymbol{q}_\ell \boldsymbol{q}_\ell)] &= -\alpha \nabla p - \Lambda_\ell \alpha \boldsymbol{e}_z + \delta K \boldsymbol{D}_{\ell a} + K \boldsymbol{D}_{\ell f}, \\ \Theta_a[(\beta \boldsymbol{q}_a)_t + \nabla.(\beta \boldsymbol{q}_a \boldsymbol{q}_a)] &= -\beta \nabla p - \Lambda_a \beta \boldsymbol{e}_z - \delta K \boldsymbol{D}_{\ell a} + \delta K \boldsymbol{D}_{af}, \\ \Theta_f[(\gamma \boldsymbol{q}_f)_t + \nabla.(\gamma \boldsymbol{q}_f \boldsymbol{q}_f)] &= -\gamma \nabla p + \nabla.\boldsymbol{\tau}_f - \Lambda_f \gamma \boldsymbol{e}_z - K \boldsymbol{D}_{\ell f} - \delta K \boldsymbol{D}_{af}, \end{aligned}$$

where $\boldsymbol{e}_z$ is a unit vector in the direction of gravity and the non-dimensional parameters Θ_k, Λ_k, δ and K are defined by

$$\Theta_k = \frac{\rho_k u_\infty^2}{E}, \quad \Lambda_k = \frac{h_i \rho_k g}{E}, \quad \delta = \frac{\rho_a \nu_a}{\rho_\ell \nu_\ell}, \quad K = \frac{\rho_\ell \nu_\ell u_\infty h_i}{E a^2},$$

with $k = \ell$, a or f.

Using the typical values given in table 1, we find that none of the values for Θ_k exceeds 4×10^{-2} and that none of the values for Λ_k exceeds 3×10^{-6}. Thus the effects

https://doi.org/10.1017/S0956792501004636 Published online by Cambridge University Press

of both macroscale inertia and gravity may be ignored (though pore inertial effects will be accounted for later). The parameter K, which measures the importance of liquid drag, is about 6, and the viscosity ratio δ is small. Hence, we neglect $\boldsymbol{D}_{\ell a}$ and $\boldsymbol{D}_{af}$ but retain the liquid-felt drag $\boldsymbol{D}_{\ell f}$. Complicating effects associated with relative permeability and capillary pressure are thus unimportant. With all the above negligibly small terms eliminated, we obtain the simplified model

$$\alpha_t + \nabla.(\alpha \boldsymbol{q}_\ell) = 0, \tag{2.16}$$

$$\beta_t + \nabla.(\beta \boldsymbol{q}_a) = 0, \tag{2.17}$$

$$\gamma_t + \nabla.(\gamma \boldsymbol{q}_f) = 0, \tag{2.18}$$

$$0 = -\alpha \nabla p + K \boldsymbol{D}_{\ell f}, \tag{2.19}$$

$$0 = -\beta \nabla p, \tag{2.20}$$

$$0 = -\gamma \nabla p + \nabla.\boldsymbol{\tau}_f - K \boldsymbol{D}_{\ell f}. \tag{2.21}$$

We have used parameter values relevant to the flow in a roll press to justify the simplifications which give rise to the model (2.16)–(2.21). However these equations are quite general, and may be applied to many different multiphase flow regimes in which (a) both inertia and gravity are negligible, (b) one of the phases (in this case, the air) has a purely passive role. One inevitable consequence of this formulation is that the flow divides naturally into saturated and unsaturated regions. In the former $\beta = 0$ and the flow is driven by a non-zero pressure gradient. In the latter $\beta > 0$, so there is no pressure gradient and the flow is hence purely kinematic.

2.4 Constitutive assumptions

To close (2.16)–(2.21) it is now necessary to make constitutive assumptions concerning the interphase drag $\boldsymbol{D}_{\ell f}$ and the felt stress $\boldsymbol{\tau}_f$. At this stage our model inevitably becomes more focused on the physical problem at hand and less widely applicable to other multiphase flows.

2.4.1 *Drag*

On dimensional grounds we suppose that the drag $\boldsymbol{D}_{\ell f}$ exerted by the felt on the liquid takes the the general form (in dimensionless variables)

$$\boldsymbol{D}_{\ell f} = -\frac{\alpha}{k(\alpha)}(\boldsymbol{q}_\ell - \boldsymbol{q}_f) G(\alpha, Re_p), \tag{2.22}$$

where $k(\alpha)$ is a dimensionless permeability and G is a dimensionless function of the liquid fraction and the pore scale Reynolds number

$$Re_p = \frac{a\,|\boldsymbol{q}_\ell - \boldsymbol{q}_f|}{\nu_\ell}.$$

Note that (2.22) applies to an isotropic porous medium; to treat anisotropy we would have to introduce a permeability tensor, whose elements in general may be functions of both α and Re_p.

The function G could be determined either by pumping water through felt in controlled

https://doi.org/10.1017/S0956792501004636 Published online by Cambridge University Press

experiments or by performing CFD calculations on a small cell that typifies the felt microstructure, but to our knowledge, at the moment no such information exists. Previous experimental evidence [8] indicates that Darcy's law $G \equiv 1$ is an adequate approximation whenever the pore Reynolds number is not too large: $Re_p \ll 86(1-\alpha)$. Otherwise the Ergun law (in which G is linear in Re_p) is preferable. In our case, if $|\boldsymbol{q}_\ell - \boldsymbol{q}_f| \sim u_\infty$ then $Re_p \approx 20$ so, to keep the equations as simple as possible in the first instance, we henceforth set $G \equiv 1$. This assumption may need to be revisited in future refinements of the model.

2.4.2 *Elasticity*

The felt is composed of a complicated juxtaposition of different nylon layers, and it is clearly impracticable to model its mechanical properties in detail. Some modelling compromise is necessary, and there are several possible approaches. In many previous poroelastic formulations (for example, Biot [2]) the solid phase is described using the theory of linear elasticity. This approach was applied to a roll press nip in Braun [4], but it seems unlikely to be very realistic because in practice (a) the strains are large, (b) the stress-strain relationship of the felt is highly nonlinear, (c) the weave of the felt means that it is inherently anisotropic. Though anisotropic linear elasticity theory could be used, a much more complicated model would result, which would address neither (a) nor (b) above. These shortcomings could be addressed only by resorting to a fully nonlinear anisotropic elasticity theory, whose attendant difficulties would seriously hinder any further analysis.

Instead, we adopt a pragmatic approach, based upon physical observations of felt behaviour. The felt has a very stiff nylon web which strongly resists any stretching. However, the weave is such that significant transverse compression can occur. Our approach is therefore to assume that the felt is 'infinitely stiff' so that its in-plane displacement is zero relative to the imposed uniform motion $u_\infty t$. Thus, the felt experiences a purely one-dimensional strain in the transverse direction (it behaves something like a mattress).

As a consequence of this approach it is no longer necessary to perform an in-plane stress balance on the felt: two components of (2.21) are replaced by the condition of zero relative displacement. Thus only one stress coefficient needs to be considered, namely τ_{fzz}, where the z-axis is normal to the centre-surface of the felt, and the strain can be characterised entirely by the solid fraction γ. The elastic behaviour is therefore encapsulated in a single scalar function $\tau_{fzz} = \mathscr{F}(\gamma)$, which in general is of the form shown in Figure 2 (for any particular felt this function can readily be established experimentally). It is worth pointing out that τ_{fzz} should be regarded as a tension force; as illustrated in figure 2, infinite tension ($\mathscr{F} \to \infty$) implies zero felt fraction, whilst the tension tends to $-\infty$ (infinite compression) when the felt fraction is unity. The elastic stress in the felt is assumed to be zero at an equilibrium solid fraction of $\gamma = \gamma_i$.

The formulation described above allows us to account for both large strains and a nonlinear stress-strain relation in a very simple manner. We anticipate, however, that a rigorous derivation of this model from nonlinear elasticity theory would be far from straightforward, and the precise assumptions to which it corresponds are therefore somewhat unclear. In addition, there are some features of the felt behaviour that we have not

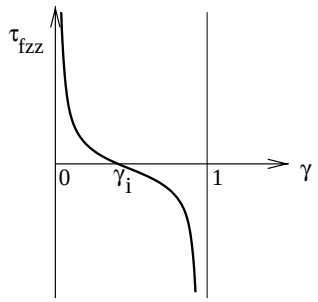

FIGURE 2. Functional form of the relationship between τ_{fzz} and γ. The solid fraction at zero stress is denoted by $\gamma = \gamma_i$.

attempted to capture. These include the slight hysteresis that is observed in experimental stress-strain measurements and the small permanent deformations of the felt that result in gradual changes in its mechanical properties.

2.5 Model statement

We are now in a position to set out our complete model for describing the motion of the felt, water and air phases. As previously stated, the flow may be partitioned into unsaturated and saturated regions. We therefore present separate systems of equations to describe each of these regimes and then briefly outline the procedure for switching between the two.

The roll press is usually run at constant speed, so we look for a steady solution and thus neglect all time derivatives. Since the rollers are extremely wide we also ignore end effects and restrict our model to two dimensions, with position vector $\boldsymbol{x} = (x, z)^T$; the x-axis points along the direction of felt motion and the z-axis in the transverse direction. The components of the water and air velocities are given by $\boldsymbol{q}_\ell = (u_\ell, w_\ell)^T$ and $\boldsymbol{q}_a = (u_a, w_a)^T$, while our treatment of the felt elasticity implies that the felt velocity is of the form $\boldsymbol{q}_f = (1, w_f)^T$.

2.5.1 *Unsaturated; $\beta > 0$*

First consider the unsaturated version of the equations (2.16)-(2.21), in which the air void fraction β is nonzero, and hence we must have $\nabla p = 0$, i.e.

$$p = \text{constant}. \tag{2.23}$$

From (2.19) we find that $\boldsymbol{D}_{\ell f} = 0$, and thus

$$w_\ell = w_f, \tag{2.24}$$

$$u_\ell = u_f = 1. \tag{2.25}$$

As noted above we only consider the z-component of (2.21), namely $(\tau_{fzz})_z = 0$, where $\tau_{fzz} = \mathscr{F}(\gamma)$. Finally, then, we arrive at three coupled equations for α, γ and w_f:

$$\alpha_x + (\alpha w_f)_z = 0, \tag{2.26}$$

https://doi.org/10.1017/S0956792501004636 Published online by Cambridge University Press

$$\gamma_x + (\gamma w_f)_z = 0, \tag{2.27}$$

$$\gamma_z = 0. \tag{2.28}$$

Notice that β is found *a posteriori* as $1 - \alpha - \gamma$; we cannot determine the air velocity $\boldsymbol{q}_a$ and never have to use the air conservation equation (2.17). This is a feature of the passive phase in such problems. In principle, $\boldsymbol{q}_a$ could be obtained by considering higher-order corrections to the model in which the small drag terms $\boldsymbol{D}_{\ell a}$ and $\boldsymbol{D}_{af}$ are included.

2.5.2 *Saturated; $\beta = 0$*

Now consider a saturated region in which $\beta = 0$, and thus

$$\alpha + \gamma = 1. \tag{2.29}$$

With a non-zero pressure gradient, the velocities of the solid and liquid phases are no longer equal so the conservation equations (2.16) and (2.18) must be written as

$$(\alpha u_\ell)_x + (\alpha w_\ell)_z = 0, \tag{2.30}$$

$$\gamma_x + (\gamma w_f)_z = 0. \tag{2.31}$$

Equation (2.19), with the drag law (2.22), gives the relative velocity via Darcy's law:

$$u_\ell = 1 - k(\alpha) p_x / K, \tag{2.32}$$

$$w_\ell = w_f - k(\alpha) p_z / K. \tag{2.33}$$

Finally, addition of (2.19) and (2.21) shows that

$$-\nabla p + \nabla . \boldsymbol{\tau}_f = 0,$$

of which we consider only the z-component, namely

$$p_z = \mathscr{F}'(\gamma)\gamma_z. \tag{2.34}$$

2.5.3 *Solution procedure*

The general methodology of solution is as follows. In unsaturated regions, (2.28) with suitable boundary conditions determines the solid fraction γ. Then with w_f found from (2.27), (2.26) becomes a single hyperbolic equation for α. Note that there is nothing in (2.23)–(2.28) to prevent the gas fraction β from becoming negative. Thus in solving for α, one must monitor $\alpha + \gamma$, and switch to the saturated regime when it reaches unity.

For saturated flow, (2.34) may be integrated to determine p. Thus γ, u_ℓ and w_ℓ can be eliminated using (2.29), (2.32) and (2.33), so that (2.30) and (2.31) provide coupled equations for α and w_f. The resulting system is nonlinear and elliptic, and the saturated model is therefore considerably harder to solve than the unsaturated version.

3 Flow in the nip

3.1 Formulation

We are now ready to apply the equations derived in the previous section to a particular geometry, shown in Figure 3, which mimics a roll press nip. In the thin-layer limit which

https://doi.org/10.1017/S0956792501004636 Published online by Cambridge University Press

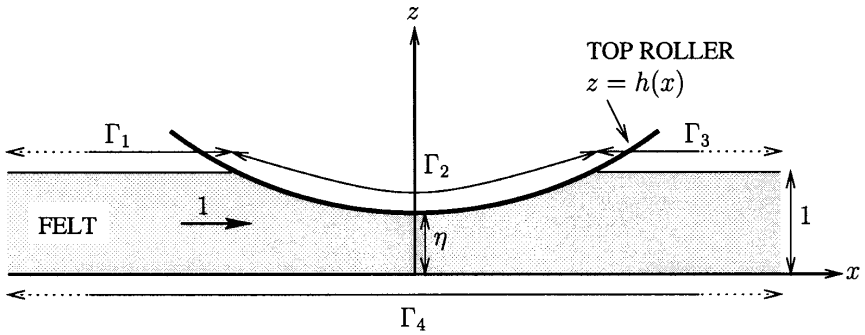

FIGURE 3. Schematic diagram of flow under a roll press nip.

we shall adopt, only the gap between the rollers is important, so no generality is lost by treating the bottom roller as flat. In dimensionless terms the felt is fed in from the left at unit speed and thickness. Since the incoming felt is unstressed, its solid fraction is the equilibrium value γ_i introduced in § 2.4.2, and the liquid and air fractions are assumed to be uniform and known. Thus before the rollers (and any upstream influence that they might generate) are encountered, we have

$$\boldsymbol{q}_\ell = \boldsymbol{q}_f = \begin{pmatrix} 1 \\ 0 \end{pmatrix}, \quad \alpha = \alpha_i, \quad \beta = 1 - \alpha_i - \gamma_i, \quad \gamma = \gamma_i.$$

As shown in Figure 3, we model the nip as the gap between two rigid surfaces at $z = 0$ and $z = h(x)$. Here h is non-dimensionalised with h_i, and thus achieves a minimum value of η at $x = 0$, where $\eta = h_0/h_i$ and h_0 is the dimensional thickness of the gap between the rollers. If the top roller is assumed to be circular, with radius $R \gg h_i$ then h can be approximated in the region of interest by

$$h = \eta + 2\epsilon^2 x^2, \quad \text{where} \quad \epsilon = \frac{1}{2}\sqrt{\frac{h_i}{R}} \ll 1. \tag{3.1}$$

The parameter η, representing the compression ratio achieved by the rollers, is expected to have a particularly important influence on the performance of the press. Since the solid fraction γ cannot exceed unity, there is a minimum possible value of the compression ratio, $\eta > \gamma_i$, while if any water is to be squeezed out at all we must have $\eta < \gamma_i + \alpha_i$. The values given in Table 1 suggest $\eta \approx 2/3$, $\epsilon \approx 0.04$.

We must now consider the conditions to be applied at each of the boundaries Γ_1–Γ_4 shown in Figure 3. Before and after the felt passes under the roller its top boundary is stress-free and assumed to be completely permeable. Thus the boundary conditions are

$$\mathscr{F} = p = 0 \quad \text{on } \Gamma_1, \Gamma_3. \tag{3.2}$$

The top roller is rigid and impermeable, which implies that

$$w_f = \frac{dh}{dx}, \quad w_\ell = u_\ell \frac{dh}{dx} \quad \text{on } \Gamma_2. \tag{3.3}$$

The bottom roller is rigid but, as described in § 1, permeable, so that water may be expelled through it. We propose a simple linear resistance law of the form $p = -Hw_\ell$

https://doi.org/10.1017/S0956792501004636 Published online by Cambridge University Press

in dimensional variables; this contains both complete permeability ($H = 0$) and total impermeability ($H \to \infty$) as limits. Thus, in dimensionless terms we have

$$w_f = 0, \quad \epsilon p = -\lambda w_\ell, \quad \text{on } \Gamma_4, \tag{3.4}$$

where

$$\lambda = \frac{\epsilon H u_\infty}{E}$$

is a dimensionless resistance parameter, which we shall assume is order one.

Finally, we note that it is possible for the pressure in the felt to be less than atmospheric pressure, in which case air and/or water may be sucked in through $z = 0$. Notice that water can only flow relative to the felt in saturated regions: in the unsaturated regime the water and felt move together while the air flows through them. Thus, at the bottom roller it is only possible in our model for either pure water or pure air to flow in and, so long as *any* air is available in the roller $z < 0$, air rather than water will be sucked into the felt. Exactly what happens in practice to water expressed into the bottom roller is unclear, but we assume it is removed rapidly enough that no water ever passes in through $z = 0$.

3.2 Thin-layer approximation

We now use the slenderness of the nip geometry to simplify the equations derived in § 2 by rescaling as follows:

$$x = \epsilon^{-1}\bar{x}, \quad w_\ell = \epsilon \bar{w}_\ell, \quad w_f = \epsilon \bar{w}_f. \tag{3.5}$$

This rescaling has no effect on the unsaturated equations (2.23)–(2.28). However the saturated model is simplified because of the order of magnitude difference between the pressure gradient terms in (2.32) and (2.33). The flow regime depends on the size of the parameter K compared with ϵ; the two distinguished limits are $K = O(1/\epsilon)$ and $K = O(\epsilon)$, of which the former appears to be more relevant to our problem. If we define

$$\kappa = \epsilon K, \tag{3.6}$$

then the values in Table 1 give $\kappa \approx 0.2$, so it is reasonable to treat κ as an order one constant. In this limit $u_\ell = u_f = 1$ to lowest order, so that there is no appreciable horizontal flow in either unsaturated or saturated domains.[1] Thus the rescaled equations and boundary conditions for the remaining unknowns are as follows:

unsaturated:

$$p = \text{constant}, \tag{3.7}$$

$$\bar{w}_\ell = \bar{w}_f, \tag{3.8}$$

$$\alpha_{\bar{x}} + \left(\alpha \bar{w}_f\right)_z = 0, \tag{3.9}$$

$$\gamma_{\bar{x}} + \left(\gamma \bar{w}_f\right)_z = 0, \tag{3.10}$$

$$\gamma_z = 0, \tag{3.11}$$

[1] This observation provides further justification of our adoption of Darcy's law in § 2.4: in our slender geometry the velocity difference between the liquid and solid phases should be estimated as $|\boldsymbol{q}_\ell - \boldsymbol{q}_f| \sim \epsilon u_\infty$ rather than u_∞, giving a pore scale Reynolds number $Re_p \approx 0.8$.

https://doi.org/10.1017/S0956792501004636 Published online by Cambridge University Press

saturated:

$$\alpha + \gamma = 1, \tag{3.12}$$

$$\alpha_{\bar{x}} + (\alpha \bar{w}_\ell)_z = 0, \tag{3.13}$$

$$\gamma_{\bar{x}} + \left(\gamma \bar{w}_f\right)_z = 0, \tag{3.14}$$

$$\bar{w}_\ell = \bar{w}_f - k(\alpha) p_z / \kappa, \tag{3.15}$$

$$p_z = \mathscr{F}'(\gamma)\gamma_z, \tag{3.16}$$

free surface conditions on $z = 1$, $\bar{x} < \bar{x}_i$ and $\bar{x} > \bar{x}_f$:

$$p = \mathscr{F} = 0, \tag{3.17}$$

top roller conditions on $z = h(\bar{x}) = \eta + 2\bar{x}^2$, $\bar{x}_i < \bar{x} < \bar{x}_f$:

$$\bar{w}_\ell = \bar{w}_f = h'(\bar{x}), \tag{3.18}$$

bottom roller conditions on $z = 0$:

$$\bar{w}_f = 0, \quad p = -\lambda \bar{w}_\ell. \tag{3.19}$$

Here $\bar{x}_i$ and $\bar{x}_f$ denote respectively the values of $\bar{x}$ at which the felt enters and exits the nip; expressions for both are given in § 3.3.

It is worth noting that the equations presented above are very much reliant on our treatment of κ and λ as order one constants. Rather different models result if either $\kappa \ll 1$ or $\lambda \gg 1$, and we briefly explore each of these limits in Appendix A. Since the remainder of the paper is devoted to the solution of equations (3.7)–(3.19), there is no further need to distinguish the rescaled variables, so we drop the over-bars henceforth.

3.3 The flow regions

As indicated schematically in Figure 4, we now decompose the felt into a number of regions in which different flow regimes exist. Region 1 refers to the felt which has yet to be squeezed between the rollers. The rollers are first encountered at the point $x = x_i$ at which $h(x_i) = 1$, i.e.

$$x_i = -\sqrt{\frac{1-\eta}{2}}, \tag{3.20}$$

and for $x > x_i$ we move into region 2. Here compression by the rollers begins, but the felt is as yet unsaturated. Saturation first occurs at a point $x = x_1$ which is to be predicted by our model (that this free boundary proves to be parallel to the z-axis is likewise a prediction of the model). For $x > x_1$ the felt is saturated and expulsion of water from $z = 0$ commences; this is denoted region 3.

Now, in $x < 0$ we have $dh/dx < 0$ so the felt is being compressed and the flow at $z = 0$ is outward. In $x > 0$ a switch in the behaviour occurs because the pressure on the felt is

https://doi.org/10.1017/S0956792501004636 Published online by Cambridge University Press

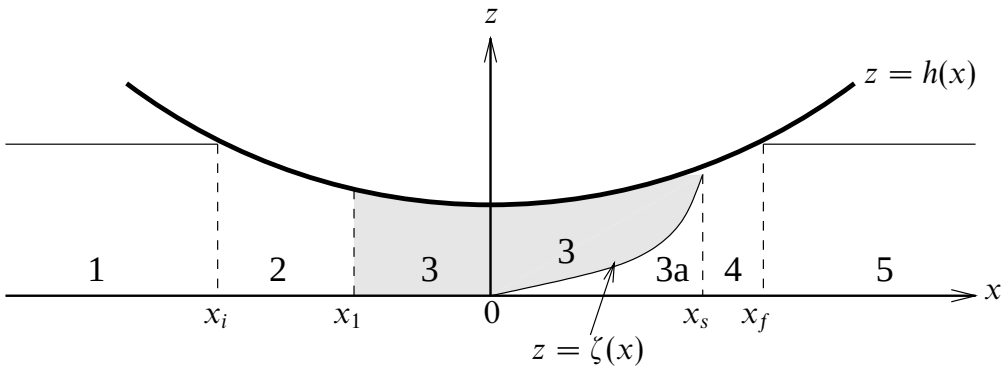

FIGURE 4. Schematic diagram of a roll press nip indicating the flow regions 1–5 defined in the text (shading indicates saturated regions).

released and it is now possible for fluid to pass in through $z = 0$. As discussed above, we assume that only air is sucked in and so there must be a region near $z = 0$, marked 3a, in which the felt is unsaturated. This is divided from a saturated domain above, which is a continuation of region 3, by a free boundary $z = \zeta(x)$. Only when the free boundary intersects with the top roller, at a point $x = x_s$ which is to be determined, is the felt unsaturated all the way through. Thereafter, in region 4, it expands with the roller up to the point $x = x_f$, at which the felt is released by the roller, and the subsequent unstressed felt is denoted region 5. It is straightforward to show that $x_f = -x_i$.

Of course, this picture of events is somewhat speculative at this stage. For example, it is not obvious *a priori* that we might not have $x_s > x_f$, in which case region 4 would not exist. Only by solving the equations in each of the regions and showing that the solutions may be successfully patched together can we confirm that the proposed structure is viable.

3.3.1 *Region 1*

In region 1 the flow is unsaturated so that equations (3.7)–(3.11) apply. The boundary conditions (3.17) imply that p and $\mathscr{F}$ are both identically zero and hence $\gamma \equiv \gamma_i$. Then (3.10) implies that w_f is independent of z, and must be identically zero, since it is zero on $z = 0$. Thus in region 1 there is no flow, and the solution is simply

$$p = 0, \quad \alpha = \alpha_i, \quad \gamma = \gamma_i, \quad w_\ell = w_f = 0. \tag{3.21}$$

Note we have assumed that the felt comes in with uniform saturation, i.e. that α_i is constant, but one could equally make α_i a specified function of z if so desired.

3.3.2 *Region 2*

In region 2 the flow is still unsaturated, but now the velocities and void fractions begin to change. The constant pressure must be zero by continuity across $x = x_i$. From (3.10), with γ independent of z and $w_f = 0$ on $z = 0$, we have

$$w_f = -\frac{z\gamma_x}{\gamma}.$$

https://doi.org/10.1017/S0956792501004636 Published online by Cambridge University Press

Then the hyperbolic equation (3.9) for α is readily solved, using the solution from region 1 as the initial condition; the solution is simply

$$\alpha = \frac{\alpha_i \gamma}{\gamma_i}.$$

Finally, we use the top roller conditions (3.18) to solve for γ. The result is

$$p = 0, \quad \alpha = \frac{\alpha_i}{h}, \quad \gamma = \frac{\gamma_i}{h}, \quad w_\ell = w_f = \frac{zh'}{h}, \tag{3.22}$$

where $h(x) = \eta + 2x^2$.

Note that since the felt is unsaturated, there is no relative flow between the water and the felt; consequently no water is lost and only air is squeezed out. More importantly, we now know where region 2 ends, namely where the air fraction reaches zero. From (3.22) we see that $\alpha + \gamma = 1$ when $h = \alpha_i + \gamma_i$, and this occurs at $x = x_1$ where

$$x_1 = \sqrt{\frac{\alpha_i + \gamma_i - \eta}{2}}. \tag{3.23}$$

As anticipated in figure 4, the saturation boundary is parallel to the z-axis; this is a consequence of our assumption that α is uniform as the felt enters the nip. Clearly we must have $\eta < \alpha_i + \gamma_i$ if saturation is to occur; otherwise region 3 does not exist and no water is expelled from the felt at all.

3.3.3 *Region 3*

In $x > x_1$ the flow is saturated so we must switch to equations (3.12)–(3.16). We begin by adding (3.13) and (3.14) and using the top roller conditions (3.18) to obtain

$$\alpha w_\ell + (1 - \alpha) w_f = h'.$$

This allows us to eliminate w_f from (3.15), whence

$$w_\ell = h' - \frac{(1 - \alpha) k(\alpha) p_z}{\kappa}.$$

With p_z given by (3.16), (3.13) can thus be turned into a single nonlinear convection-diffusion equation for α:

$$\alpha_x + h'\alpha_z = [D(\alpha)\alpha_z]_z \quad \text{where} \quad D(\alpha) = -\frac{\alpha(1 - \alpha) k(\alpha) \mathscr{F}'(1 - \alpha)}{\kappa}. \tag{3.24}$$

Recall from Figure 2 that $\mathscr{F}'$ is negative, so the diffusion coefficient is a positive function of α, whose behaviour depends on the functional forms of $\mathscr{F}$ and k; typically $D \to \infty$ as $\alpha \to 1$ while as $\alpha \to 0$, D may tend to infinity, zero or a finite value.

Equation (3.24) requires one initial and two boundary conditions. The initial condition comes from patching with region 2, and the boundary conditions from substituting our expression for w_ℓ into (3.18) and (3.19) while using (3.16):

$$\alpha = \frac{\alpha_i}{\alpha_i + \gamma_i} \quad \text{at} \quad x = x_1, \tag{3.25}$$

$$\alpha_z = 0 \quad \text{at} \quad z = h(x), \tag{3.26}$$

$$\alpha k(\alpha) \mathscr{F}'(1 - \alpha) \alpha_z = \kappa h'(x) \quad \text{at} \quad z = 0. \tag{3.27}$$

https://doi.org/10.1017/S0956792501004636 Published online by Cambridge University Press

The problem (3.24)–(3.27) now appears to be correctly specified, but must be solved numerically and this is carried out in § 4. Notice that integration of (3.24) with respect to z and application of the boundary conditions gives rise to the identity

$$\int_0^{h(x)} \alpha \, dz \equiv h(x) - \gamma_i, \tag{3.28}$$

which represents total conservation of felt (and of water). An attractive numerical approach is to use (3.28) in place of the bottom roller condition (3.27), the advantage being that such a scheme automatically conserves both felt and water.

Once α has been found, all other dependent variables can readily be determined via

$$p = \mathscr{F} - \mathscr{F}|_{z=0} - \frac{\lambda h'}{\alpha(x,0)}, \tag{3.29}$$

$$w_\ell = h' + \frac{(1-\alpha)k(\alpha)\mathscr{F}'(1-\alpha)\alpha_z}{\kappa}, \tag{3.30}$$

$$w_f = h' - \frac{\alpha k(\alpha)\mathscr{F}'(1-\alpha)\alpha_z}{\kappa}. \tag{3.31}$$

Notice that the resistance parameter λ only appears in the expression (3.29) for the pressure; it has no effect on the problem for α.

Unlike regions 1 and 2, we do not yet know where region 3 ends, and it is not clear how far into $x > 0$ (3.24) should be solved. From (3.29) we can see that p changes sign on the bottom roller when $h' = 0$, i.e. at the nip. Thus, as anticipated, in $x > 0$ air is sucked in through the bottom roller, giving rise to an unsaturated region 3a, which is separated from the saturated region 3 by a free boundary denoted $z = \zeta(x)$. It should be noted, however, that the derivations of the diffusion equation (3.24) and the upper boundary condition (3.26) do not rely on the conditions applied on $z = 0$. Thus they continue to hold in $x > 0$, and it is only the lower boundary condition that must be replaced.

3.3.4 *Region 3a*

In region 3a we return to the unsaturated equations. The pressure is constant and therefore zero, since $z = 0$ is assumed to be exposed to atmospheric pressure. From (3.11) we know that γ is independent of z, and it is convenient to define

$$\gamma = g(x) \tag{3.32}$$

in this region. Just as in region 2, the water and felt velocities are found to be

$$w_\ell = w_f = -\frac{z g'(x)}{g(x)}. \tag{3.33}$$

Again we obtain from (3.9) a hyperbolic equation for α, namely

$$\alpha_x = \frac{g'(x)}{g(x)} (z\alpha)_z, \tag{3.34}$$

whose general solution is

$$\alpha = \frac{1}{z} f(z g(x)), \tag{3.35}$$

where the function f is, as yet, unknown.

https://doi.org/10.1017/S0956792501004636 Published online by Cambridge University Press

It is rather more awkward here than was the case in region 2 to fit the initial conditions for α and thus determine the arbitrary function f. On the boundary $z = \zeta(x)$ of the saturated region we have $\beta = 0$ and therefore $\alpha = 1 - g(x)$, so f satisfies the equation

$$(1 - g(x))\zeta(x) = f(\zeta(x)g(x)). \tag{3.36}$$

However, as yet neither the free boundary $\zeta(x)$ nor the function $g(x)$ has been determined. The information that closes (3.36) can only be obtained by solving the saturated problem in $z > \zeta(x)$ and applying conditions of continuity across $z = \zeta$, as described below. Once ζ and g are known, f is given by (3.36), α by (3.35) and the velocities by (3.33).

3.3.5 *Free boundary conditions*

We must now consider the continuity conditions to be applied on the free boundary $z = \zeta(x)$ which divides regions 3 and 3a. Since the phases are in contact at the free boundary, the pressure must be continuous and indeed zero, because it is zero in region 3a. Then a stress balance on the interface implies that $\mathscr{F}$ is continuous, as must therefore be γ. We have assumed that $\beta = 0$ on either side of the interface, and thus α must likewise be continuous. Then mass conservation of felt and of water implies that w_f and w_ℓ are both continuous.

We use this last observation, with w_ℓ and w_f given by (3.30) and (3.31) in region 3 and by (3.33) in region 3a, to deduce two conditions on the free boundary, namely

$$\alpha_z = 0 \quad \text{on } z = \zeta^+$$

(notice that this can be applied only on the region 3 side of the interface since α_z is not in general continuous) and

$$h'(x) = -\frac{\zeta(x)g'(x)}{g(x)}.$$

In this latter condition g can replaced with α by using

$$g(x) = 1 - \alpha(x, \zeta(x)). \tag{3.37}$$

3.3.6 *Region 3 continued*

We may now summarise. In region 3 we have the well-posed problem (3.24)–(3.27) to solve in $x_1 \leqslant x \leqslant 0$, $0 \leqslant z \leqslant h(x)$. For $x > 0$ we introduce the free boundary $z = \zeta(x)$. In the saturated region $z > \zeta$ we have to solve

$$\alpha_x + h'\alpha_z = [D(\alpha)\alpha_z]_z, \tag{3.38}$$

with α continuous across $x = 0$, D as defined in (3.24) and the boundary conditions

$$\alpha_z = 0 \quad \text{at} \quad z = h(x), \tag{3.39}$$

$$\alpha_z = 0 \quad \text{at} \quad z = \zeta(x), \tag{3.40}$$

$$(1 - \alpha)h'(x) = \alpha_x\zeta(x) \quad \text{at} \quad z = \zeta(x). \tag{3.41}$$

In principle this determines both α in region 3 and the location of the free boundary

https://doi.org/10.1017/S0956792501004636 Published online by Cambridge University Press

$\zeta(x)$. As for (3.28), we may replace the final boundary condition (3.41) by an integral constraint,

$$\int_{\zeta(x)}^{h(x)} \alpha \, dz \equiv h(x) - \gamma_i - \zeta(x)\alpha(x, \zeta(x)), \tag{3.42}$$

representing conservation of felt, and thereby formulate a conservative numerical scheme.

The velocities in this region are then given by (3.30) and (3.31), and the pressure by

$$p = \mathscr{F} - \mathscr{F}|_{z=\zeta}, \tag{3.43}$$

using the fact that it is zero on $z = \zeta$.

Once α is known, (3.37) gives $g(x)$ and (3.36) may then be used to determine f and thus the complete solution in region 3a. Alternatively, (3.36) may be reformulated in an integral form,

$$\int_0^{g(x)\zeta(x)} \frac{f(y)}{y} \, dy \equiv (1 - g(x))\zeta(x) + \eta - h(x), \tag{3.44}$$

which identically conserves water. It is worth pointing out that in either case our proposed solution procedure relies on the implicit equation (3.36) possessing a unique solution, i.e. on the free boundary being nowhere parallel to the characteristics in region 3a. Although it seems at least plausible, and is supported by our numerical results in § 4, we have no *a priori* guarantee that this is the case. We return to this point in § 3.4.

3.3.7 *Region 4*

The solution in region 3a is valid only until the free boundary hits the top roller. Let us assume that this happens at $x = x_s$, so that $\zeta(x_s) = h(x_s)$, and that at this point $\alpha(x_s, z) = \alpha_s(z)$. Both x_s and $\alpha_s(z)$ are to be found numerically. Region 4 is unsaturated, and its only role is to allow air to re-enter the gaps left by the water that has been squeezed out. Just as in region 3a we have γ independent of z and

$$w_\ell = w_f = -\frac{z\gamma_x}{\gamma}.$$

Now we apply the kinematic condition (3.18) on $z = h$ to obtain

$$\gamma = \frac{\gamma_i}{h},$$

exactly as in region 2. Thus the hyperbolic equation (3.9) for α reads

$$\alpha_x + \frac{h'(x)}{h(x)} (z\alpha)_z = 0,$$

and the solution, with $\alpha = \alpha_s$ at $x = x_s$, is

$$\alpha = \frac{h(x_s)}{h(x)} \alpha_s \left(\frac{z h(x_s)}{h(x)} \right). \tag{3.45}$$

3.3.8 *Region 5*

In region 5 the flow is again unsaturated and unstressed so we have $h = 1$, $p = 0$, $\mathscr{F} = 0$ and hence $\gamma = \gamma_i$. (Note that one could also consider examples where the felt enters the

https://doi.org/10.1017/S0956792501004636 Published online by Cambridge University Press

roller with a non-zero stress, so that the final and initial felt thicknesses are not the same.) There is no flow, $w_\ell = w_f = 0$, and thus no further water either enters or leaves the felt. We may read off from (3.45) α_o and β_o, the outgoing liquid and air fractions:

$$\alpha_o(z) = h(x_s)\alpha_s(zh(x_s)), \quad \beta_o(z) = 1 - \gamma_i - \alpha_o(z). \tag{3.46}$$

This is the most important prediction of our model, and should enable us to quantify the effectiveness of the roll press. Recall that the paper is located in a thin layer on top of the felt, so the water content near $z = 1$ may be of particular interest. This outgoing state of the felt might also be used as the initial condition for a model of the felt's subsequent passage through the next stage in the process.

Interestingly, since there is no significant horizontal flow in the thin-layer limit, the *total* amount of water removed from the felt is known exactly. At the minimum point $x = 0$ we have $h = \eta$, the air fraction is zero, the total felt fraction is γ_i/η and the total water fraction is therefore $1 - \gamma_i/\eta$. As the felt expands in $x > 0$, no water flows into or out of the felt, and thus at $x = x_f$, where $h = 1$, the total water fraction is

$$\int_0^1 \alpha_o(z)\,dz = \eta - \gamma_i, \tag{3.47}$$

assuming η is in the range $\gamma_i < \eta < \gamma_i + \alpha_i$. Thus if only the total amount of water left in the felt as it exits the nip is required, there is no need to perform the numerical calculations described in § 4.

3.4 Well-posedness of the free-boundary problem

In this section we have shown how the flow may be broken down into a number of distinct regions in which different models apply. We have obtained expressions which determine all the flow properties – the velocity and fraction of each phase and the pressure – in each region, once the following have been carried out.

(i) The boundary-value problem (3.24)–(3.27) must be solved for α in $x_1 < x < 0$.

(ii) The free-boundary problem (3.38)–(3.41) must then be solved for α and $\zeta(x)$ in $x > 0$, using $\alpha(0, z)$ just calculated as the initial condition.

(iii) Finally, given $\zeta(x)$ and $g(x) = \alpha(x, \zeta(x))$ we have to solve (3.36) for the function f.

Numerical methods to implement each of these and sample solutions will be presented in § 4. Before doing so it is worthwhile to discuss in slightly more detail the assumptions which led to the free-boundary problem (3.38)–(3.41), the circumstances under which those assumptions might fail and the possible difficulties which might arise in solving (3.36) for f.

Physically, the free boundary $z = \zeta(x)$ is a saturation front that is receding relative to the moving felt. The way this occurs is that the water-logged felt expands and air flows in to fill the resulting gaps; the saturation boundary marks the felt which has only just expanded to the point that air can get in. For this reason the air fraction is continuous across such a boundary, as assumed in § 3.3.

In the unsaturated region 3a, the characteristics of the hyperbolic equation (3.34) are felt streamlines. Thus the saturation front is retreating with respect to the moving felt,

https://doi.org/10.1017/S0956792501004636 Published online by Cambridge University Press

as described above, so long as the characteristics travel *out* of $z = \zeta(x)$. It can readily be shown that the characteristics pass through $z = \zeta(x)$ with slope $h'(x)$, so for the front to be everywhere receding, we require the free boundary to be steeper than the roller at each point. If this condition is satisfied then we can also be sure that (3.36) specifies f uniquely.

Now, if we ever reached a point at which $\zeta' = h'$, the equation (3.36) for f would become indeterminate. Physically, this would correspond to transition from a retreating to an advancing saturation front. At any subsequent points where $\zeta' < h'$, the characteristics travel *into* $z = \zeta(x)$, and the assumptions which led to our free-boundary problem are no longer valid. Across an advancing saturation front, the air fraction is *not* continuous in general, and hence neither is α nor w_ℓ. Instead we would have to impose the jump condition

$$\zeta'(x) = \frac{[\alpha w_\ell]^+_-}{[\alpha]^+_-},$$

where $[\cdot]^+_-$ represents the jump across the free boundary. On the unsaturated side α is in principle known on the characteristics passing into $z = \zeta$.

The theory outlined above in § 3.3 is based on the implicit assumption that such a transition does not occur. Intuitively, it seems unlikely that the saturation front would ever begin to advance while the felt is expanding, and no such difficulties have been encountered in any of our numerical calculations, but we have not as yet been able to prove that it is impossible.

3.5 Inner layer at $x = x_1$

Another aspect of our solution which warrants further discussion is the behaviour near $x = x_1$, which divides regions 2 and 3. It is clear from (3.22), (3.30) and (3.31) that the velocity components w_ℓ and w_f are discontinuous across $x = x_1$. This may seem surprising at first glance, but in fact w_ℓ and w_f are allowed to be discontinuous across any line $x =$ constant. Of more concern is the fact that, if the resistance parameter λ is nonzero, (3.22) and (3.29) imply that the pressure is discontinuous across $x = x_1$, which is certainly not physical. This is a consequence of our thin-layer limit, and is resolved by considering an inner layer near $x = x_1$, in which the pressure gradient drives a significant horizontal flow.

The appropriate rescaling is

$$x = x_1 + \epsilon\xi, \quad \text{where, recall,} \quad \eta + 2x_1^2 = \alpha_i + \gamma_i.$$

The saturation boundary (which need not in general be straight) is denoted by $\xi = \chi(z)$. Thus we have to solve the unsaturated equations in $\xi < \chi$ and the saturated equations in $\xi > \chi$, while imposing continuity conditions on $\xi = \chi$. These comprise continuity of pressure and of stress,

$$[p]^+_- = \chi' [\gamma]^+_- = 0,$$

and conservation laws for felt and for water,

$$\left[\gamma(1 - \epsilon\chi' w_f)\right]^+_- = \left[\alpha(u_\ell - \epsilon\chi' w_\ell)\right]^+_- = 0.$$

https://doi.org/10.1017/S0956792501004636 Published online by Cambridge University Press

The inner expansions take the forms

$$\alpha \sim \frac{\alpha_i}{\alpha_i+\gamma_i} + \epsilon\alpha_1 + \ldots, \quad \gamma \sim \frac{\gamma_i}{\alpha_i+\gamma_i} + \epsilon\gamma_1 + \ldots, \quad w_\ell \sim w_{\ell 0} + \epsilon w_{\ell 1} + \ldots,$$

and so forth, outside boundary layers near $z = 0$ and $z = h$; we omit the details of the analysis here. It transpires that the free boundary is straight to lowest order (χ_0 is constant) and the unsaturated solution is that already obtained in region 2. In the saturated region $\xi > \chi$ we find

$$\alpha_1 = -\gamma_1 = \frac{\alpha_i\gamma_i k_0}{\kappa(\alpha_i+\gamma_i)^2} p_0'(\xi),$$
$$w_{\ell 0} = w_{f0} = -\frac{\alpha_i}{\lambda(\alpha_i+\gamma_i)} p_0(\xi) + \frac{z\alpha_i k_0}{\kappa(\alpha_i+\gamma_i)} p_0''(\xi),$$

where k_0 is shorthand for $k(\alpha_i/(\alpha_i+\gamma_i))$, the leading-order pressure is given by

$$p_0(\xi) = -\frac{4\lambda x_1(\alpha_i+\gamma_i)}{\alpha_i}\left(1 - e^{\xi/\chi_0 - 1}\right),$$

and the free boundary by

$$\chi_0 = -\sqrt{\frac{\lambda k_0(\alpha_i+\gamma_i)}{\kappa}}.$$

Thus this inner solution gives a smooth transition in the pressure from zero on the saturation boundary to the constant value predicted on $x = x_1$ by (3.29). The main effect of a nonzero resistance on the bottom roller is to move the saturation boundary a small distance $\epsilon\chi_0$ upstream. This local behaviour has no influence on the solution procedure outlined in § 3.3.

4 Results

We now present example calculations based on the theory detailed in § 3. To start with we outline numerical methods designed to solve the various equations without making specific choices for such parameters as the elastic properties of the felt. The methods given may thus be used to conduct 'numerical experiments' in which the parameters within the theory are varied. For the purpose of illustration, we then present some example calculations based on particularly simple constitutive laws.

4.1 Numerical methods

A numerical method of solution is needed to calculate the behaviour of $\alpha(x, z)$. The remaining variables such as γ, p, and the vertical velocities may be calculated fairly simply once α is known. Within the thin-layer approximation, α evolves in the positive x direction from x_i to x_f according to its continuity equation

$$\alpha_x + (\alpha w_\ell)_z = 0, \tag{4.1}$$

where the vertical velocity of the liquid, w_ℓ, is related to α and possibly its z-derivative depending on whether the region is saturated or not. A numerical treatment of this equation can be broken down into three parts: (a) the interval $x_1 \leqslant x \leqslant 0$ in which the

https://doi.org/10.1017/S0956792501004636 Published online by Cambridge University Press

felt is completely saturated, (b) the interval $0 < x < x_s$ in which the felt is saturated for $\zeta(x) < z < h(x)$, and (c) the interval $x_s \leqslant x \leqslant x_f$ in which the felt is unsaturated. (A numerical method is not needed for the unsaturated region $x_i \leqslant x < x_1$.) A conservative, second-order accurate, finite-volume numerical scheme will be developed to determine α for each of these intervals. This is done so that a discrete form of the integral conservation form given in (3.28) is preserved exactly in the numerical solution.

We begin with a discussion of the numerical method for the interval $x_1 < x \leqslant 0$. For this saturated region, α evolves according to (4.1) with

$$w_\ell = h' - D(\alpha)\frac{\alpha_z}{\alpha}, \tag{4.2}$$

where the diffusivity $D(\alpha)$ is defined in (3.24). The equation for α is a convection-diffusion equation as mentioned previously with an initial condition at $x = x_1$ given by (3.25) and boundary conditions at $z = h(x)$ and $z = 0$ given by (3.26) and (3.27), respectively.

For numerical convenience, we introduce a change of variables, $z = h(x)y$, so that the interval $0 < z < h(x)$ becomes $0 < y < 1$. In the variables (x, y), the conservation equation for α becomes

$$(h\alpha)_x + \left[\alpha\left(w_\ell - yh'\right)\right]_y = 0. \tag{4.3}$$

We define grid lines $y_j = j\Delta y$ for $j = 0, 1, \ldots, n$ with $\Delta y = 1/n$, and let

$$U_j(x) = \frac{1}{\Delta y}\int_{y_{j-1}}^{y_j} h(x)\alpha(x, y)\, dy.$$

Point values for α are related to U_j by

$$\alpha(x, y_{j-1/2}) = U_j(x)/h(x) + O(\Delta y^2),$$

and thus $U_j(x)$ may be regarded as the numerical solution we seek. A discrete conservation equation for U_j may be obtained by integrating (4.3) over a grid cell of width Δy and of length Δx. Using the divergence theorem, we find

$$U_j(x + \Delta x) = U_j(x) - \frac{\Delta x}{\Delta y}\left(F_j(x) - F_{j-1}(x)\right), \tag{4.4}$$

where $F_j(x)$ is a flux defined by

$$F_j(x) = \frac{1}{\Delta x}\int_x^{x+\Delta x} \left[\alpha\left(w_\ell - yh'\right)\right]\Big|_{y=y_j} dx. \tag{4.5}$$

An approximation is needed to relate F_j to the solution U_j. For this saturated region, we use the following centred, second-order accurate approximation:

$$\tilde{F}_j(x) = \tilde{\alpha}(x, y_j)(1 - y_j)\tilde{h}'(x) - D(\tilde{\alpha}(x, y_j))\tilde{\alpha}_z(x, y_j), \tag{4.6}$$

where (4.2) has been used to eliminate w_ℓ, and

$$\tilde{\alpha}(x, y_j) = \frac{1}{4}\left[\frac{U_{j+1}(x + \Delta x) + U_j(x + \Delta x)}{h(x + \Delta x)} + \frac{U_{j+1}(x) + U_j(x)}{h(x)}\right],$$

$$\tilde{\alpha}_z(x, y_j) = \frac{1}{2\Delta y}\left[\frac{U_{j+1}(x + \Delta x) - U_j(x + \Delta x)}{h^2(x + \Delta x)} + \frac{U_{j+1}(x) - U_j(x)}{h^2(x)}\right],$$

https://doi.org/10.1017/S0956792501004636 Published online by Cambridge University Press

and

$$\tilde{h}'(x) = \frac{h(x+\Delta x) - h(x)}{\Delta x}.$$

The initial condition gives $U_j(x_1) = \text{constant} = \alpha_i$ and the boundary conditions imply

$$\tilde{F}_0(x) = \frac{h(x+\Delta x) - h(x)}{\Delta x} \qquad \text{and} \qquad \tilde{F}_n(x) = 0.$$

If $U_j(x)$, $j = 1, 2, \ldots, n$, is known and a value for the step size, Δx, is chosen, then the conservation equation (4.4) with the approximate flux (4.6) provides a set of n nonlinear algebraic equations for $U_j(x+\Delta x)$, $j = 1, 2, \ldots, n$. These equations are readily solved using Newton's method. This procedure may be repeated to obtain U_j at discrete values of x throughout the saturated region $x_1 \leqslant x \leqslant 0$. Further,

$$\begin{aligned}\int_0^{h(x+\Delta x)} \alpha(x+\Delta x, z)\, dz &= \Delta y \sum_{j=1}^{n} U_j(x+\Delta x) \\ &= \Delta y \sum_{j=1}^{n} U_j(x) - \Delta x \sum_{j=1}^{n} \left(\tilde{F}_j(x) - \tilde{F}_{j-1}(x)\right) \\ &= \int_0^{h(x)} \alpha(x, z)\, dz + h(x+\Delta x) - h(x)\end{aligned}$$

so that

$$\int_0^{h(0)} \alpha(0, z)\, dz = \int_0^{h(x_1)} \alpha(x_1, z)\, dz + h(0) - h(x_1) = \eta - \gamma_i\,.$$

The exact expression for the total amount of water squeezed out by the nip is preserved by the numerical solution.

We now consider the interval $0 < x < x_s$ in which the felt is saturated for $\zeta(x) < z < h(x)$ and unsaturated for $0 < z < \zeta(x)$, where $z = \zeta(x)$ is the saturation boundary which must be determined as part of the problem. On both sides of the saturation boundary, continuity of α holds so that we may use the conservation form given in (4.4) throughout the interval with an appropriate choice for w_ℓ used in (4.5) depending on whether y_j is greater than or less than $\zeta(x)/h(x)$. Let us assume that the saturation boundary intersects the grid line $x = x_{m-1}$ at $y = y_{m-1}$ for an integer $m \in [1, n-1]$ as shown in Figure 5 and that $\Delta x_m = x_m - x_{m-1}$ is chosen such that the saturation boundary intersects $x = x_m$ at $y = y_m$ as well. The grid cells $m+1 \leqslant j \leqslant n$ lie above the saturation boundary so that the numerical scheme outlined previously applies with the exception that $\tilde{F}_j$ in (4.6) for $j = m$ is replaced by

$$\tilde{F}_m(x_{m-1}) = \hat{\alpha}(x_{m-1}, y_m)(1 - y_m)\tilde{h}'(x_{m-1}) - D(\hat{\alpha}(x_{m-1}, y_m))\hat{\alpha}_z(x_{m-1}, y_m) \tag{4.7}$$

where

$$\hat{\alpha}(x_{m-1}, y_m) = \frac{1}{4}\left[\frac{2U_{m+1}(x_m)}{h(x_m)} + \frac{U_{m+1}(x_{m-1}) + U_m(x_{m-1})}{h(x_{m-1})}\right]$$

and

$$\hat{\alpha}_z(x_{m-1}, y_m) = \frac{1}{2\Delta y}\left[\frac{U_{m+1}(x_{m-1}) - U_m(x_{m-1})}{h^2(x_{m-1})}\right],$$

noting that $\alpha_z = 0$ on $z = \zeta^+$. An additional equation may be derived from the boundary

https://doi.org/10.1017/S0956792501004636 Published online by Cambridge University Press

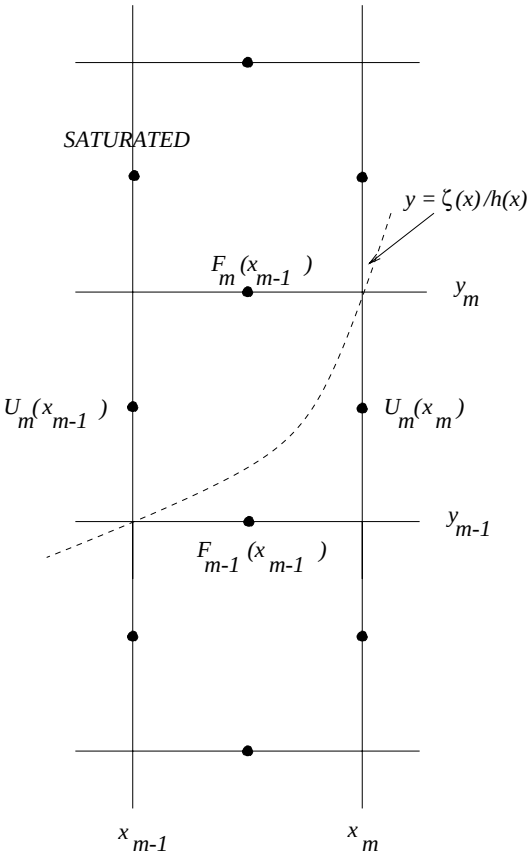

FIGURE 5. Numerical grid near saturation boundary.

condition (3.41) in order to specify the correct value of Δx_m. This boundary condition may be written as

$$(\ln h)' + \eta(x)(\ln(1-\alpha))_x = 0$$

where $\eta = \zeta/h$ and then approximated by

$$\ln\left[\frac{h(x_m)}{h(x_{m-1})}\right] + y_{m-1/2}\ln\left[\frac{1-U_{m+1}(x_m)/h(x_m)}{1-U_m(x_{m-1})/h(x_{m-1})}\right] = 0$$

which provides an additional equation needed to determine Δx_m. We now have $n-m+1$ nonlinear algebraic equations for the $n-m+1$ unknowns $\{U_{m+1}(x_m),\ldots,U_n(x_m),\Delta x_m\}$. These equations may be solved using Newton's method.

The remaining values $U_j(x_m)$, $j=1,\ldots,m$, are obtained using (4.4) and a different approximate flux suitable for an unsaturated region. In the unsaturated region 3a, w_ℓ is given by (3.33). This equation may be used in (4.5) to obtain an approximate flux

$$\tilde{F}_j(x_{m-1}) = y_j c(x_{m-1}) U_j^\star(x_{m-1}) \tag{4.8}$$

where

$$c(x_{m-1}) = \frac{1}{\Delta x_m}\ln\left[\frac{h(x_m)-U_{m+1}(x_m)}{h(x_{m-1})-U_m(x_{m-1})}\right]$$

https://doi.org/10.1017/S0956792501004636 Published online by Cambridge University Press

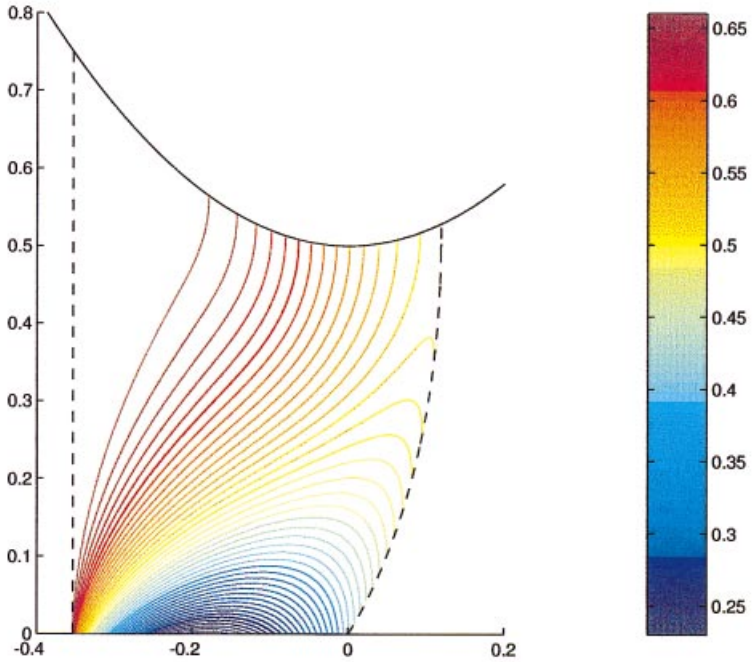

FIGURE 6. Water content in the saturated region for $\alpha_i = 0.5$, $\kappa = 1$.

and

$$U_j^\star(x_{m-1}) = \frac{1}{2}\left(U_{j+1}(x_m) + U_j(x_m)\right) + \frac{\Delta x_m c(x_{m-1})}{2\Delta y}\left(y_{j+1/2}U_{j+1}(x_m) - y_{j-1/2}U_j(x_m)\right)$$

The value for $c(x_{m-1})$ is determined by the previous solution at the saturation boundary. This value is the wave speed for the hyperbolic equation for α in the unsaturated region 3a. The value for $U^\star$ involves a 'backwards' Lax-Friedrichs step which leads to a second-order accurate flux. Typically, this step would be taken in the forwards direction thus giving an explicit scheme, however for our problem finite differences cannot be taken across the saturation boundary so that a backwards step is more convenient. A set of m linear algebraic equations are given by (4.4) for $1 \leqslant j \leqslant m$ with $\Delta x = \Delta x_m$ (as determined previously), $\tilde{F}_j$ given by (4.8) for $1 \leqslant j \leqslant m-1$, $\tilde{F}_m$ given by (4.7), and $\tilde{F}_0 = 0$ (noting that there is no flux of water at $z = 0$ for $x > 0$). The solution of these equations determine the remaining values for $U_j(x_m)$ in the unsaturated region. It is noted that while the saturation boundary divides the mth cell, conservation of α given by (4.4) still holds, and thus

$$\int_0^{h(x_m)} \alpha(x_m, z)\, dz = \Delta y \sum_{j=1}^{n} U_j(x_m) = \Delta y \sum_{j=1}^{n} U_j(x_{m-1}) = \int_0^{h(x_{m-1})} \alpha(x_{m-1}, z)\, dz$$

so that the total amount of water in the felt is conserved for $0 < x < x_s$.

The general procedure for the mixed saturated/unsaturated region on the interval $0 < x < x_s$ is to start with the initial values $U_j(0)$, $j = 1, \ldots, n$ given by the calculation of the fully saturated region and $m = 1$, and then compute saturated values $U_j(x_1)$,

https://doi.org/10.1017/S0956792501004636 Published online by Cambridge University Press

$j = 2,\ldots,n$, and the step size Δx_1 using Newton's method. The remained unsaturated value, $U_1(x_1)$, is found by solving a linear equation. We then set $m = 2$ and first compute the solution in the saturated region and the step size, Δx_2, followed by a calculation of the remaining two unsaturated values. This procedure continues with increasing m until $m = n - 1$ at which point only one saturated value remains. The values of Δx_m approach zero monotonically so that a reasonable approximation for x_s is x_{n-1}.

It is noted that unlike the fully saturated region $x_1 \leqslant x \leqslant 0$ where there is no fixed choice for Δx (a reasonable choice is $\Delta x \simeq \Delta y$ for accuracy), the constraint that the saturation boundary intersects specific vertices on the grid chooses a unique Δx_m for each $m \in [1, n-1]$. This particular construct is convenient and works well for this problem because $\Delta x_m \leqslant \Delta x_1 \simeq .3\Delta y$ for a typical calculation. Conversely, if the slope of the saturation boundary had been very small so that $\Delta x_1/\Delta y$ had been very large, then a different numerical approach would have been required to obtain a reasonable accuracy.

The final region to consider is the fully unsaturated region for $x_s \leqslant x \leqslant x_f$. In this region

$$w_\ell = \frac{zh'}{h}$$

so that $F_j(x) = 0$ exactly and (4.4) reduces to $U_j(x + \Delta x) = U_j(x)$ for any choice of Δx. The solution is constant on grid lines $y = y_j$ and its value may be found from the last solution value calculated from the mixed saturated/unsaturated region.

4.2 Example calculations

To illustrate the overall numerical method, we now make some choices for the various parameters in the system. We begin with geometry and set $\eta = 1/2$ in all our calculations, so that the upper roller shape is given by $h(x) = 1/2 + 2x^2$ and the felt is compressed by the rollers to half of its original thickness. Next, we consider the incoming state of the three phase air-liquid-felt system. Our choice of η implies that the felt first touches the upper roller at $x = x_i = -1/2$. The incoming fraction of air is taken to be $\beta_i = 1/4$ while the incoming fraction of water given by α_i will be varied to study the behaviour of the system. Thus, the incoming fraction of felt is $\gamma_i = 1 - \alpha_i - \beta_i = 3/4 - \alpha_i$.

Finally, we need to make assumptions regarding the flow through and the elastic properties of the felt. Since the calculations presented here are intended to be primarily illustrative, we make the simplest possible choices which are probably not particularly realistic. We set the permeability $k(\alpha)$ to be constant; this constant may without loss of generality be set to unity if it is understood that the dimensional permeability is accounted for by an effective pore size a. The elastic behaviour of the felt is determined by $\mathscr{F}$, whose qualitative form is shown in Figure 2. Near $\gamma = \gamma_i$ we may use the linear approximation

$$\mathscr{F} = \sigma(\gamma_i - \gamma)$$

where $\sigma = -\mathscr{F}'(\gamma_i)$ is a positive constant. Away from γ_i we expect significant deviation from this linear fit, but we shall accept this approximation for all values of γ for the purposes of our illustrative example. We may set $\sigma = 1$ by a suitable choice of the dimensional elastic modulus E. Hence, in view of the above assumptions concerning k

https://doi.org/10.1017/S0956792501004636 Published online by Cambridge University Press

and $\mathscr{F}$, a single dimensionless parameter, namely

$$\kappa = \frac{\rho_\ell v_\ell u_\infty h_i^{3/2}}{2Ea^2\sqrt{R}},$$

encapsulates all the effects of varying (a) the liquid properties, (b) the feed speed, (c) the permeability and stiffness of the felt, and (d) the roller size. It will be useful to think of κ as an elastic parameter: decreasing κ corresponds to increasing the felt stiffness.

The uniform incoming state from region 1 provides starting information for the solution in region 2. Using the formulae in § 3.3.2 and the choices for η and the incoming fractions of air and water given above, we find

$$\alpha = \frac{\alpha_i}{1/2 + 2x^2}, \qquad \beta = 1 - \frac{3/4}{1/2 + 2x^2}, \qquad \gamma = \frac{3/4 - \alpha_i}{1/2 + 2x^2}$$

$$w_\ell = w_f = \frac{4xz}{1/2 + 2x^2}, \qquad p = 0.$$

These formulae apply for $-1/2 \leqslant x \leqslant x_1$, where $x_1 = -1/\sqrt{8}$ is the value of x when $\beta = 0$ and the felt becomes saturated. At this point, the fractions of water and felt are

$$\alpha_1 = \frac{4\alpha_i}{3}, \qquad \gamma_1 = 1 - \frac{4\alpha_i}{3}$$

which are greater than their incoming values. The behaviour of α in the remaining regions and the saturation boundary may be found using the numerical approach outlined previously.

Figure 6 shows contours of the fraction of water in the saturated region for the choice $\alpha_i = 0.5$ and $\kappa = 1.0$. The colour bar to the right of the figure indicates the value for α on each contour. The interval in α between contour lines is 0.01. The black curve at the top of the figure gives the shape of the roller and the dashed curves to the left and right mark the boundaries of the saturated region, and in particular the dashed curve to the right is the free boundary $z = \zeta(x)$. As expected, the maximum fraction of water occurs at the left saturation boundary, where $\alpha = \alpha_1 = 2/3$. For $x > x_1$, water is squeezed out of the saturated felt, so that α decreases with increasing x, at least initially. Near the roller, $z = h(x)$, 'diffusion' dominates and the fraction of water decreases monotonically. Near the flat surface $z = 0$ there is a rapid decrease in α followed by a gentler increase towards the nip, $x = 0$. The initial decrease is in response to the geometric convergence of the roller. As the slope of the roller approaches zero near the nip, this convergence eases while 'diffusion' tends to equilibrate the water content, causing α to increase along $z = 0$.

Figures 7(a) and 7(b) give contours of α for the cases $\alpha_i = 0.5$, $\kappa = 0.5$ and $\alpha_i = 0.4$, $\kappa = 0.5$, respectively. A smaller value of κ models a more rigid felt which, as seen by comparing figures 6 and 7(a), results in a smaller reduction in α near $z = 0$. The effect of decreasing α_i, and thus decreasing α_1, can be seen by comparing the solutions in Figures 7(a) and 7(b). The solution in Figure 7(b) shows a significant reduction in the minimum value of α along $z = 0$. In fact numerical experiments with even smaller values of α_i (holding κ fixed) indicate that it is possible for this minimum to become zero, implying that all water has been squeezed out of the felt. A nonlinear elastic law like that shown in Figure 2 would give infinite stress as the solid fraction approaches unity; in practice

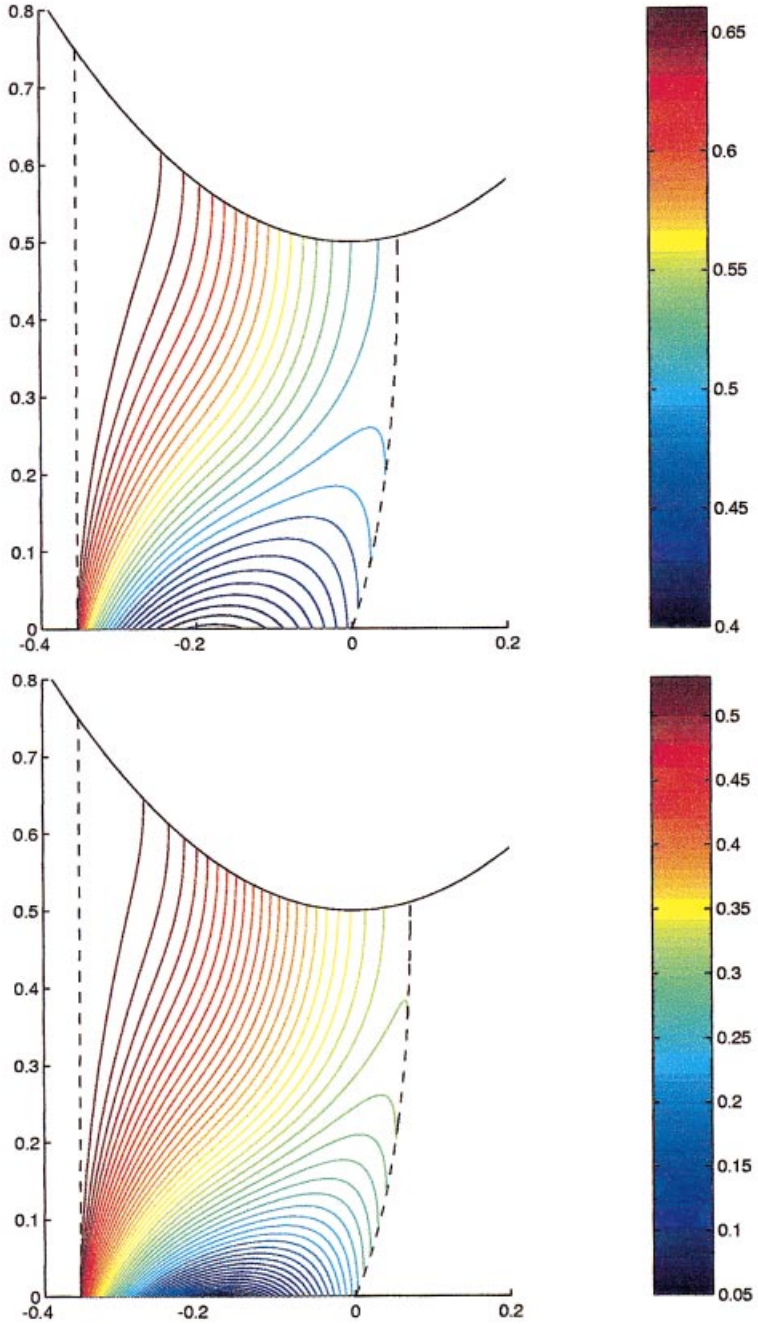

FIGURE 7. Water content in the saturated region for (a) $\alpha_i = 0.5$, $\kappa = 0.5$ and (b) $\alpha_i = 0.4$, $\kappa = 0.5$.

we might expect the machine to jam if too much compression is attempted. In any case, our mathematical model (and numerical method) would require modification to continue the solution beyond that point.

The liquid and felt velocities, w_ℓ and w_f, respectively, can be worked out from $\alpha(x, z)$

https://doi.org/10.1017/S0956792501004636 Published online by Cambridge University Press

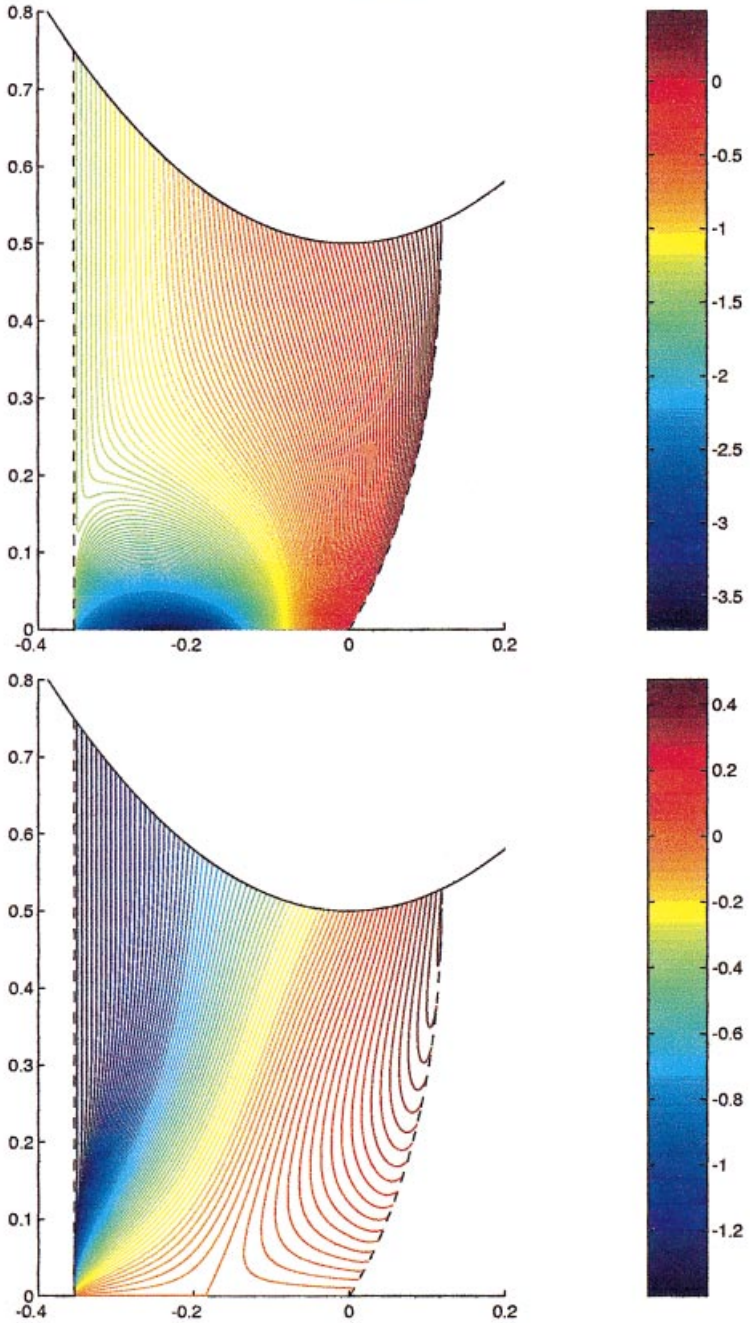

FIGURE 8. Vertical velocities in the saturated region for $\alpha_i = 0.5$ and $\kappa = 1$: (a) liquid velocity and (b) felt velocity.

https://doi.org/10.1017/S0956792501004636 Published online by Cambridge University Press

in region 3 using (3.30) and (3.31). These velocities are shown in Figure 8 for the case $\alpha_i = 0.5$ and $\kappa = 1.0$, corresponding to Figure 6. The liquid velocity has a minimum along $z = 0$ where the water leaves the felt most rapidly. The felt velocity is constrained to be zero along $z = 0$. On the roller, both w_ℓ and w_f are equal to $h'(x)$, in accordance with the boundary condition there.

Once the velocities are determined, the pressure in the saturated region is given by (3.29) and (3.43). Figure 9 shows the pressure for the case $\alpha_i = 0.5$, $\kappa = 1.0$ and $\lambda = 0$, so that the bottom roller is completely permeable. For this choice of λ, the pressure is zero along $z = 0$ which matches the value at the saturation boundaries.

Finally, we show the behaviour of α for the entire interval $x_i \leqslant x \leqslant x_f$ in Figure 10 for the case $\alpha_i = 0.5$ and $\kappa = 1.0$. This plot shows the variations in α in the unsaturated regions prior to and following the saturated region 3. Of particular interest in the plot is the fraction of liquid at $x = 1/2$, which increases monotonically from 0.1755 at $z = 0$ to 0.2782 at $z = 1$, a value significantly less than the incoming value of 0.5. The total water fraction at $x = 1/2$ is $\eta - \gamma_i = 0.25$.

5 Conclusions

We have proposed a model for the flow of water and air through a deformable porous medium in a roll press nip. The model was initially formulated in some generality, before specific assumptions were made to reduce the complexity of the working equations. Thus a hierarchy of models was presented, starting with (2.1)–(2.6) which lie at the heart of almost any study of multiphase flow. Various standard closure assumptions were made to arrive at the system (2.10)–(2.15), which is in principle closed once constitutive relations for stress and interphase drag have been specified.

The next level of specification was to use the physical characteristics of the system under consideration to decide which terms in the model could be neglected. This resulted in (2.16)–(2.21), which seem to apply quite generally to three-phase poroelastic problems in which inertia is negligible and one phase is passive. A characteristic of such flows is that they divide into unsaturated and saturated regions, depending on whether the air fraction is positive or zero, with a different set of equations to be applied in each case.

Constitutive relations specific to our problem were proposed, resulting in the systems (2.23)–(2.28) for unsaturated flow and (2.29)–(2.34) for saturated flow. For the drag between the liquid and solid phases we used Darcy's law. We acknowledged that there may be circumstances under which pore-scale inertia cannot be neglected and indicated how such effects may be incorporated in our model by use of Ergun's law. As an elastic constitutive law we assumed that the felt is compressible only in one direction, as is suggested by experimental observations. This simple-minded approach produces equations that are amenable to further analysis while allowing for elastic nonlinearity and large strains.

Finally, our model was further simplified by exploiting the slender geometry of a roll press nip, resulting in the equations (3.7)–(3.19) whose solution was then obtained by a combination of analytical and numerical means. One might ask whether taking this slender limit produced a significant simplification of the model, since only one term (the horizontal pressure gradient) was eliminated from the equations, which were still complicated enough to require numerical treatment. The great advantage of our approach

is that the equation (3.24) to be solved in the saturated region becomes parabolic; in the general case it is elliptic. Thus there are no upstream influences, and in § 3.3 we described how one can march downstream treating each flow region in turn.

In one of these regions (region 3) it is necessary to solve a nonlinear convection-diffusion equation with a free boundary and we presented a numerical method to achieve this. We illustrated the method with some example calculations. Since we do not at present possess details of realistic felt properties, very simple constitutive assumptions were employed in our simulations, but we were still able to observe many of the important features of the squeezing process. In particular we showed that one can readily predict the water content of the felt as it leaves the rollers, which is the most important outcome of any modelling of the roll press.

Although we aim to have proposed a coherent model for the flow in a roll press nip, much work remains to be carried out. The following areas of further study suggest themselves.

- Many of the sub-models within our model are open to question and may need to be refined to better reflect the physical characteristics of the system. Particular attention should be given to the elastic behaviour of the felt and to the water-felt drag law (for example, it is arguably inconsistent to model the felt as isotropic so far as permeability is concerned but elastically anisotropic).
- As noted in the text, it is not obvious that the patching together of the different regions discussed in § 3.3 will always be successful, although no such difficulties have been encountered in our simulations. A more rigorous mathematical analysis might shed further light on the well-posedness of the problem as a whole.
- There is scope for much more detailed asymptotic analysis of the various flow regions, in particular those where the thin-layer limit is locally nonuniform.
- The paper is not treated explicitly in our model. To do so we would have to regard the solid sheet entering the rollers as consisting of two layers with distinct properties.
- More information is needed concerning the boundary conditions that are satisfied on the bottom roller. In particular, we need to know the circumstances under which air may be sucked into the felt and how much resistance there is to the flow of water into the bottom roller.
- A more detailed simulation of the press would require the state of the water-loaded felt as it approaches the roller to be properly specified.

Acknowledgements

The authors are grateful to the organising committee of the Fifteenth Annual Workshop on Mathematical Problems in Industry at the University of Delaware in June 1999, at which the problem was originally brought to their attention. They are also indebted to Dr John Skelton of Albany International who presented the problem at the Workshop and provided valuable insight. PDH was partially funded by a Junior Research Fellowship from Christ Church, Oxford.

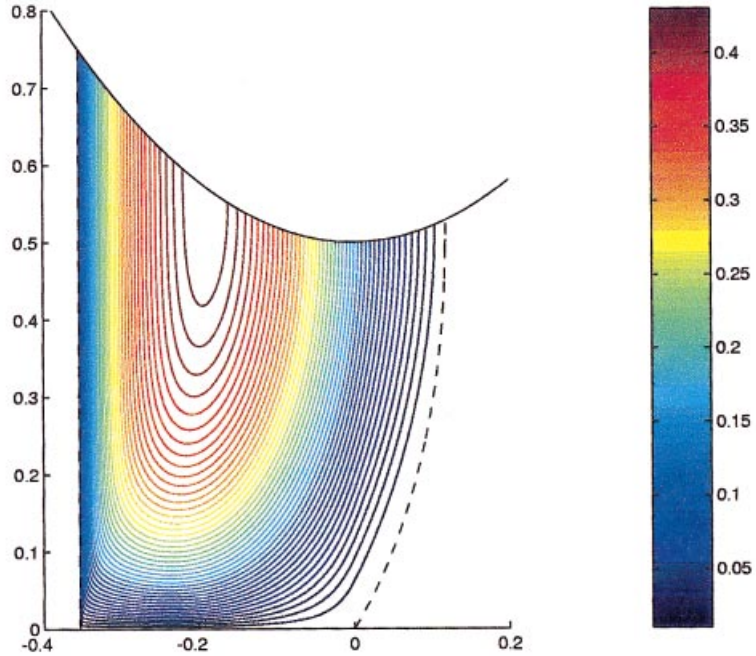

FIGURE 9. Pressure in the saturated region for $\alpha_i = 0.5$ and $\kappa = 1$.

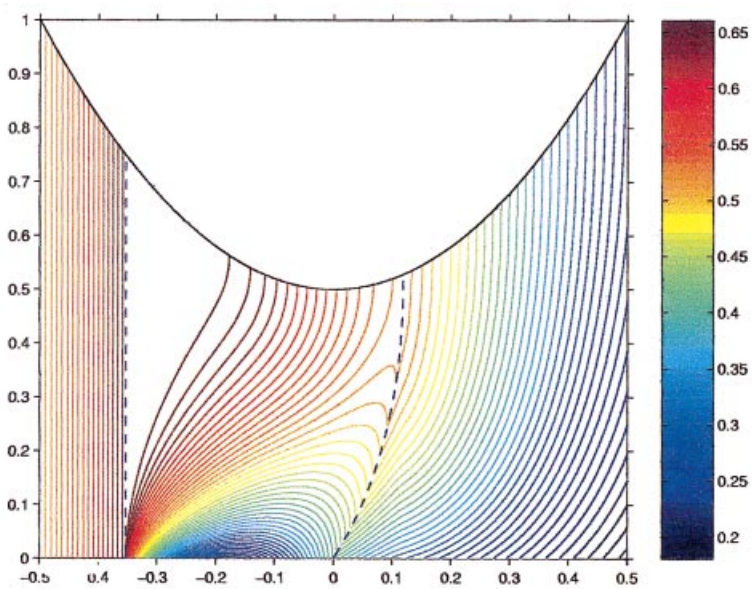

FIGURE 10. Water content for $\alpha_i = 0.5$ and $\kappa = 1$.

https://doi.org/10.1017/S0956792501004636 Published online by Cambridge University Press

Appendix A Other distinguished limits

When making a thin-layer approximation in § 3, we had to take a view on the orders of magnitude of the parameters

$$K = \frac{\rho_\ell v_\ell u_\infty h_i}{E a^2} \quad \text{and} \quad \lambda = \frac{\epsilon H u_\infty}{E}$$

in the limit $\epsilon \to 0$. The model (3.7)–(3.19), subsequently solved in § 4, was obtained under the assumptions $K = O(1/\epsilon)$, $\lambda = O(1)$. The first of these is consistent with the data given in Table 1, but one should be aware that these values are only approximate, and a modest change in the felt properties (i.e. in E and a) could make K small. At the moment our information about the permeability of the bottom roller is very sketchy, so our assumption about the size of λ is essentially a guess based on the presumption that ideally the bottom roller offers very little resistance to the passage of water.

It is of interest, then, to examine the effects on our model of varying the sizes of both K and λ. Two distinguished limits remain to consider. We start in § A.1 with $K = O(1/\epsilon)$, as in the text, but a much higher resistance on the bottom roller: $\lambda = O(1/\epsilon^2)$. Then in § A.2 we consider a felt with higher permeability and/or lower stiffness such that $K = O(\epsilon)$, in which case only the limit $\lambda = O(1)$ is distinguished. The unsaturated equations are affected by none of these rescalings, so in each case we present the equations and boundary conditions for a saturated region between a permeable base $z = 0$ and an impermeable roller $z = h(x)$ (corresponding to region 3 in Figure 4).

A.1 $K = O(1/\epsilon)$, $\lambda = O(1/\epsilon^2)$

In this regime the increased resistance of the bottom roller results in much higher water pressures, and it is necessary to rescale p. Thus we define

$$\kappa = \epsilon K, \quad \Lambda = \epsilon^2 \lambda, \quad P = \epsilon^2 p,$$

each of which is then assumed to be order one. The saturated equations become, to lowest order,

$$\alpha + \gamma = 1, \tag{A 1}$$

$$(\alpha u_\ell)_x + (\alpha w_\ell)_z = 0, \tag{A 2}$$

$$\gamma_x + (\gamma w_f)_z = 0, \tag{A 3}$$

$$u_\ell = 1 - k(\alpha) P_x / \kappa, \tag{A 4}$$

$$w_\ell = w_f - k(\alpha) \mathscr{F}'(\gamma) \gamma_z / \kappa, \tag{A 5}$$

$$P_z = 0, \tag{A 6}$$

with boundary conditions

$$w_f = h', \quad w_\ell = u_\ell h' \quad \text{on} \quad z = h(x), \tag{A 7}$$

$$w_f = 0, \quad P = -\Lambda w_\ell \quad \text{on} \quad z = 0. \tag{A 8}$$

https://doi.org/10.1017/S0956792501004636 Published online by Cambridge University Press

A possible approach to this system is as follows. First use (A 3), (A 5), (A 6) and (A 8) to obtain

$$w_f = -\frac{1}{\gamma}\int_0^z \gamma_x(x,\tilde{z})\,d\tilde{z}, \quad P(x) = \frac{\Lambda}{\kappa}\left[k(\alpha)\mathscr{F}'(\gamma)\gamma_z\right]_{z=0}.$$

Thus, by using (A 4), (A 2) can be turned into a single nonlocal parabolic PDE for α (or γ). This system appears to be somewhat more awkward to deal with than the equations solved in the text, largely because here there is significant horizontal flow of water ($u_\ell \not\sim 1$).

A.2 $K = O(\epsilon)$, $\lambda = O(1)$

Now we suppose the parameter $\mathscr{K} = K/\epsilon$ and λ are both order one. In this limit there is no need to rescale p and the leading-order saturated equations and boundary conditions are

$$\alpha + \gamma = 1, \tag{A 9}$$

$$(\alpha u_\ell)_x + (\alpha w_\ell)_z = 0, \tag{A 10}$$

$$\gamma_x + (\gamma w_f)_z = 0, \tag{A 11}$$

$$u_\ell = 1 - k(\alpha)p_x/\mathscr{K}, \tag{A 12}$$

$$0 = p_z, \tag{A 13}$$

$$p_z = \mathscr{F}'(\gamma)\gamma_z, \tag{A 14}$$

$$w_f = h', \quad w_\ell = u_\ell h' \quad \text{on} \quad z = h(x), \tag{A 15}$$

$$w_f = 0, \quad p = -\lambda w_\ell \quad \text{on} \quad z = 0. \tag{A 16}$$

From (A 9), (A 12), (A 13) and (A 14) we see that p, α, γ and u_ℓ are all independent of z. It follows from conservation of felt (A 11) that

$$\gamma(x) = \frac{\gamma_i}{h(x)}, \quad w_f = \frac{zh'(x)}{h(x)},$$

and from conservation of water (A 10), with the boundary conditions on $z = 0$ and $z = h$, that

$$p = -\frac{\lambda}{\alpha}\frac{d}{dx}(\alpha u_\ell h).$$

Substitution for α and u_ℓ reduces this to a second-order ODE for $p(x)$. This limit is similar to classical lubrication theory, with liquid squeezed out horizontally by the rollers. Both upstream and downstream boundary conditions must be imposed on p, in contrast with the parabolic problem solved in the text.

Finally we note that if $K = O(\epsilon)$ and $\lambda = O(1/\epsilon^2)$, the leading-order model turns out to be identical to (A 9)–(A 16), except that the bottom roller has infinite resistance: the second equation in (A 16) is replaced by $w_\ell = 0$ on $z = 0$. Thus, this regime can be obtained simply by applying the limit $\lambda \to \infty$ to the equations above.

References

[1] Atkin, R. J. & Craine, R. E. (1976) Continuum theories of mixtures: basic theory and historical development. *Q. J. Mech. Appl. Math.* **29**, 210–244.

https://doi.org/10.1017/S0956792501004636 Published online by Cambridge University Press

[2] Biot, M. A. (1941) General theory of three-dimensional consolidation. *J. Appl. Phys.* **12**, 155–164.
[3] Biot, M. A. (1955) Theory of elasticity and consolidation for a porous anisotropic solid. *J. Appl. Phys.* **26**, 182–185.
[4] Braun, R. (ed.) (1999) The fifteenth annual workshop on mathematical problems in industry, *Final Report*, University of Delaware, Newark, DE.
[5] Cheng, A. H.-D. & Detourney, E. (1998) On singular integral equations and fundamental solutions of poroelasticity. *Int. J. Solids Structures*, **35**, 4521–4555.
[6] Drew, D. A. (1983) Mathematical-modeling of 2-phase flow. *Ann. Rev. Fluid Mech.* **15**, 261–291.
[7] Drew, D. A. & Wood, R. T. (1985) Overview and taxonomy of models and methods for workshop on two-phase flow fundamentals. *National Bureau of Standards Report*, Gaithersburg, MD.
[8] Ergun, S. (1952) Fluid flow through packed columns. *Chem. Eng. Prog.* **48**, 89–94.
[9] Fitt, A. D. (1996) Mixed systems of conservation laws in industrial mathematical modelling. *Surv. Math. Ind.* **6**, 21–53.
[10] Ishii, M. (1975) *Thermo-fluid Dynamic Theory of Two-Phase Flows*. Eyrolles, Paris.
[11] Jiang, Q. & Rajapakse, R. K. N. D. (1994) On coupled heat and moisture transfer in deformable porous-media. *Q. J. Mech. Appl. Math.* **47**, 53–68.
[12] Kenyon, D. E. (1979) A mathematical model of water flux through aortic tissue. *Bull. Math. Biol.* **41**, 79–90.
[13] Lai, W. M. & Mow, V. C. (1980) Drag induced compression of articular cartilage during a permeation experiment. *Biorheology* **17**, 111–123.
[14] Preziosi, L., Joseph, D. D. & Beavers, G. S. (1996) Infiltration of initially dry, deformable porous media. *Int. J. Multiphase Flow*, **22**, 1205–1222.
[15] Reese, R. A. (1999) *The Paper Machine Wet Press Manual (4th ed)*. TAPPI Press (Technical Association of the Pulp and Paper Industry).
[16] Spiegelman, M. (1993) Flow in deformable porous-media. 1. Simple analysis. *J. Fluid Mech.* **247**, 17–38.
[17] Terzaghi, K. (1925) *Erdbaumechanik*. Vienna: Franz Deuticke.